

# Herpes Simplex Virus Type 1 (HSV-1)–Induced Retinitis Following Herpes Simplex Encephalitis: Indications for Brain-to-Eye Transmission of HSV-1

Jeroen Maertzdorf, MSc,<sup>1</sup> Allegonda Van der Lelij, PhD,<sup>2</sup> G. Seerp Baarsma, MD,<sup>3</sup> Albert D. M. E. Osterhaus PhD,<sup>1</sup> and Georges M. G. M. Verjans, PhD<sup>3</sup>

**Herpes simplex encephalitis is a severe neurological disease with high mortality and morbidity rates. Reactivated herpes simplex virus type 1 (HSV-1) can cause relapses and might even spread to the retina, where it can induce a potentially blinding eye disease, known as acute retinal necrosis. In the present study, the HSV-1 strains in the brain and eye of 2 patients with acute retinal necrosis following an episode of herpes simplex encephalitis were genotyped. The HSV-1 strains in both the brain and eye were identical in each patient, but they differed interindividually. The data suggest brain-to-eye transmission of HSV-1 in these patients.**

Ann Neurol 2001;49:104–106

Herpes simplex encephalitis (HSE), caused by an infection of the brain by herpes simplex virus (HSV) is a severe disease with high mortality and morbidity rates.<sup>1</sup> Reactivation and neuronal translocation of HSV can result in relapses of HSE or new infections at anatomically different sites, such as the eye. Clinical data suggest that HSE may be a risk factor for the development of acute retinal necrosis (ARN), a rapidly progressing and potentially blinding eye disease induced by HSV.<sup>2–4</sup>

Two patients with HSE in whom ARN developed later in life were included in this study. The HSV-1 strains involved in both disease manifestations of each patient were genotyped using a newly developed polymerase chain reaction (PCR) method<sup>5</sup> and subsequent nucleotide sequence analyses. The data indicate that in both patients HSE and ARN were caused by a single HSV-1 strain, suggesting transneuronal spread of the virus from brain to eye.

From the <sup>1</sup>Department of Virology, Erasmus University, and <sup>2</sup>Rotterdam Eye Hospital, Rotterdam and <sup>3</sup>Department of Ophthalmology, Leiden University Medical Center, Leiden, The Netherlands.

Received Jun 12, 2000, and in revised form Jul 31. Accepted for publication Aug 7, 2000.

Address correspondence to Dr Verjans, Department of Virology, Erasmus University, PO Box 1738, 3000 DR Rotterdam, The Netherlands.

## Patients and Methods

### Patients

Patient 1 was a 68-year-old man who had been admitted to the hospital in a somnolent state. A viral encephalitis was suspected, and computed tomographic scans showed a hypodensity in the right temporal region. A cerebrospinal fluid (CSF) sample showed leukocyte counts of  $73 \times 10^6/L$ . Diagnosis of HSE was confirmed by detection of HSV-1 DNA, determined by PCR using virus-specific primers as described<sup>6</sup> and HSV-specific antibodies in the CSF. Intravenous treatment with 10 mg/kg acyclovir three times daily for 2 weeks resulted in slow recovery. However, 9 months after discharge from the hospital, he experienced a unilateral acute decrease of VISUAL ACUITY. The diagnosis of ARN was made on clinical grounds and confirmed by detection of HSV-1 DNA and local HSV-specific antibody production in the aqueous humor as described previously.<sup>6</sup> Again the patient was treated with acyclovir, and maintenance therapy with valacyclovir resulted in a slight improvement, with a remaining visual acuity of 0.5.

Patient 2 was a 64-year-old woman hospitalized because of progressive headache with vomiting and aphasia. Scans showed a hypodense and space-occupying process in the left temporal region. A CSF sample showed a leukocyte count of  $44 \times 10^6/L$ , and the diagnosis of HSE was confirmed by detection of HSV-1 DNA<sup>6</sup> and HSV-specific antibodies in the CSF. A slow recovery was achieved after intravenous treatment with 10 mg/kg acyclovir three times daily for 2 weeks. Only 10 days after being discharged from the hospital, this patient experienced unilaterally decreased visual acuity. ARN was diagnosed 2 weeks later. An aqueous humor sample contained HSV-1 DNA as determined by PCR, whereas no local HSV-specific antibody production could be detected.<sup>6</sup> Again, this patient was given antiviral treatment with acyclovir. However, despite maintenance therapy, the remaining visual acuity was only finger counting at 3 meters.

### HSV-1 Strain Differentiation

Isolation of DNA from the CSF and aqueous humor samples from both patients, taken for diagnostic purposes, was performed as described previously.<sup>6</sup> The HSV-1 strains in these samples were genotyped with a recently developed PCR-based DNA fingerprint assay that allows the rapid and accurate discrimination of up to 92% of unrelated HSV-1 strains.<sup>5</sup> The assay is based on the amplification of hypervariable regions within the HSV-1 genes US1 and US12. These regions contain strain-to-strain differences in the number of DNA repeats, termed reiteration IV (ReIV),<sup>7</sup> resulting in variable amplicon lengths between HSV-1 strains. Size and specificity of the PCR products were determined on an agarose gel and Southern blotting with ReIV-specific probes. Nucleotide sequence analysis of gel-purified HSV-1 US12 gene amplicons was performed with both PCR primers on a Perkin Elmer (Foster City, CA) automated sequencer using a commercially available kit according to the manufacturer's instructions (DYEnamic ET Terminator; Amersham Pharmacia, Cleveland, OH).

## Results

The CSF- and aqueous humor–derived HSV-1 strains from both patients were genotyped using a recently developed PCR assay.<sup>5</sup> Although they were different



## Discussion

Several studies have reported on the development of HSV-induced ARN following an episode of HSE.<sup>2-4</sup> It has been hypothesized that the induction of ARN in these patients was due to reactivation of latent HSV within the brain and subsequent infection of the retina. Studies on the experimental ARN mouse model have provided evidence for this assumption. Herein, intraocular inoculation of mice with HSV-1 resulted in infection of the brain and subsequent ARN in the contralateral eye. The virus was shown to reach the retina of the contralateral eye by transaxonal spread through the optic nerve.<sup>8</sup>

Here, 2 ARN patients with a previous episode of HSE were studied to determine whether a similar mode of brain-to-eye transmission of HSV-1 had occurred. Detailed genotypic analyses of the HSV-1 strains located in the brain and eye samples from these patients strongly suggest that the viruses found in both anatomical sites of each patient were identical but differed interindividually. To our knowledge, this is the first study to provide molecular evidence that a single HSV-1 strain can cause HSE and subsequently ARN in a single individual. Analogous to the ARN mouse model, this suggests that the virus may have spread from the brain to the eye, probably through the optic nerve.

The potential of HSV-1 to establish latency in the brain<sup>9</sup> and reactivate from neural cells poses a lifetime threat of recurrent infections. Our findings should alert neurologists to the possibility that HSE may be followed by ARN, since only prompt and specialized medical care may prevent the loss of sight in such patients. Patients recovering from HSV brain infections should be closely monitored for viral eye infections, probably for the rest of their lives.

---

This study was funded in part by the Dr F. P. Fischer Stichting (J.M.) and SWOO, Rotterdamse Vereniging Blindenbelangen, and stichting HOF (G.M.G.M.V.).

---

## References

1. Whitley RJ. Herpes simplex virus infections of the central nervous system: a review. *Am J Med* 1988;85:61-67.
2. Pavesio CE, Conrad DK, Mc Cluskey PJ, et al. Delayed acute retinal necrosis after herpetic encephalitis. *Br J Ophthalmol* 1997;81:415-420.
3. Levinson RD, Reidy R, Chiu MT. Acute retinal necrosis after neonatal herpes encephalitis. *Br J Ophthalmol* 1999;83:123-124.
4. Ganatra JB, Chandler D, Santos C, et al. Viral causes of the acute retinal necrosis syndrome. *Am J Ophthalmol* 2000;129:166-172.
5. Maertzdorf J, Remeijer L, Van der Lelij A, et al. Amplification of reiterated sequences of herpes simplex virus type 1 (HSV-1) genome to discriminate between clinical HSV-1 isolates. *J Clin Microbiol* 1999;37:3518-3523.
6. Doornenbal P, Baarsma GS, Quint WGV, et al. Diagnostic as-

says in cytomegalovirus retinitis: detection of herpesvirus by simultaneous application of the polymerase chain reaction and local antibody analysis on ocular fluid. *Br J Ophthalmol* 1996;80:235-240.

7. Umene K, Yoshida M. Reiterated sequences of herpes simplex virus type 1 (HSV-1) genome can serve as physical markers for the differentiation of HSV-1 strains. *Arch Virol* 1989;106:281-299.
8. Matsubara A, Atherton SS. Spread of HSV-1 to the suprachiasmatic nuclei and retina in T cell depleted BALB/c mice. *J Neuroimmunol* 1997;80:165-171.
9. Nicoll JAR, Love S, Kinrade E. Distribution of herpes simplex virus DNA in the brains of human long-term survivors of encephalitis. *Neuroscience Letters* 1993;157:215-218.

## A Novel mtDNA Mutation in the ND5 Subunit of Complex I in Two MELAS Patients

Paola Corona, MSc, Carlo Antozzi, MD, Franco Carrara, BSc, Ludovico D'Incerti, MD, Eleonora Lamantea, MSc, Valeria Tiranti, PhD, and Massimo Zeviani, MD, PhD

---

**We identified a novel heteroplasmic mutation in the mitochondrial DNA gene encoding the ND5 subunit of complex I. This mutation (13514A→G) hits the same codon affected by a previously reported mitochondrial encephalomyopathy, lactic acidosis, and strokelike episodes (MELAS)-associated mutation (13513G→A), but the amino acid replacement is different (D393G vs D393N). The 13514A→G mutation was found in two unrelated MELAS-like patients. However, in contrast to typical MELAS, lactic acidosis was absent or mild and the muscle biopsy was morphologically normal. Strongly positive correlation between the percentage of heteroplasmy and defective activity of complex I was found in cybrids. We found an additional 13513G→A-positive case, affected by a progressive mitochondrial encephalomyopathy. Our results clearly demonstrate that the amino acid position D393 is crucial for the function of complex I. Search for D393 mutations should be part of the routine screening for mitochondrial disorders.**

*Ann Neurol* 2001;49:106-110

---

From the Istituto Nazionale Neurologico "C. Besta," Milano, Italy. Received Mar 27, 2000, and in revised form Aug 14. Accepted for publication Aug 15, 2000.

Address correspondence to Dr Zeviani, Division of Biochemistry and Genetics, Istituto Nazionale Neurologico "C. Besta," via Celoria, 11 Milano 20133, Italy. E-mail: zeviani@tin.it

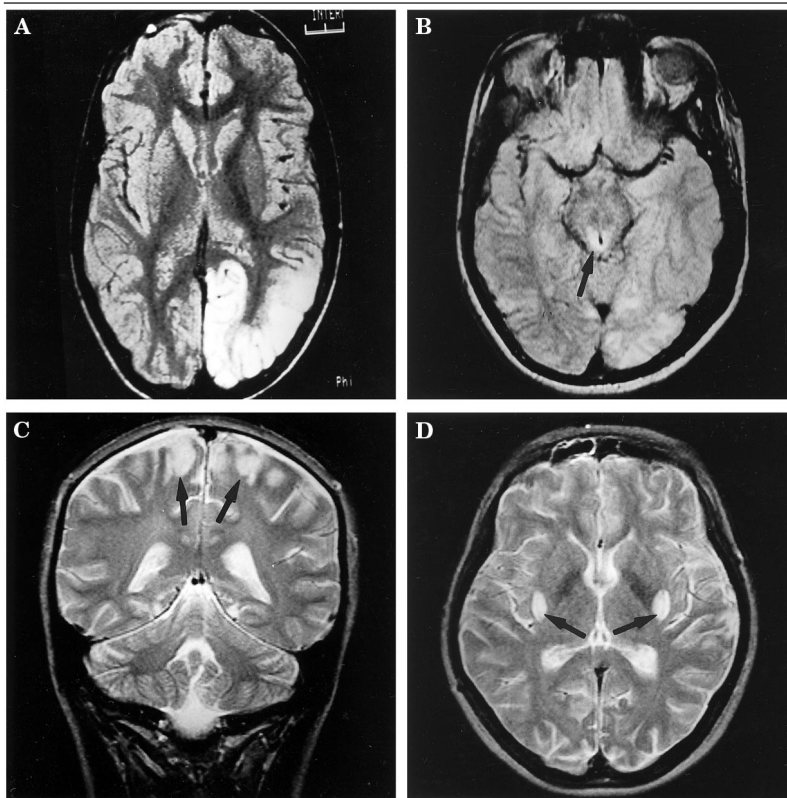


*Fig 1. Brain magnetic resonance image of Patients 1 and 2. (A) Axial proton-density weighted image of Patient 1. Note the hyperintense signal in the left occipital and posterior temporal lobes. (B) Axial proton-density weighted image of Patient 1 6 years after the study shown in (A). The hyperintense lesion in the occipital and posterior temporal lobes is reduced, whereas a new periaqueductal hyperintensity area has appeared (arrow). (C) Coronal T2-weighted image of Patient 2. Note the presence of several cortical hyperintense areas in the parietal lobes (arrows). (D) Axial T2-weighted image of Patient 2. Note the symmetrical hyperintense areas in the posterior basal ganglia (arrows).*

The association between mitochondrial encephalomyopathy, lactic acidosis, and strokelike episodes (MELAS) (MIM no. 540000), and the 3243G→A mutation in the mitochondrial DNA (mtDNA) tRNA<sup>Leu(UUR)</sup> gene<sup>1</sup> is well-established in all ethnic backgrounds. However, not all MELAS cases carry this mutation.<sup>2</sup> On the other hand, approximately 20% of 3243G→A-positive patients are affected by other syndromes such as progressive external ophthalmoplegia<sup>3</sup> and deafness-diabetes mellitus syndrome.<sup>4</sup> Moreover, MELAS is a heterogeneous clinical entity and can include, besides the obligatory signs indicated in the acronym, virtually any neurological abnormality described in mitochondrial disorders.<sup>5</sup> In a molecular investigation on several 3243G→A-negative MELAS-like cases, we identified a novel heteroplasmic mutation in the mtDNA gene encoding subunit ND5 of complex I.

## Case Reports

### Patient 1

Patient 1 is a 26-year-old male. At age 13 years, scintillating scotomas in the right visual field were followed by headache and several brief episodes of loss of consciousness. A brain magnetic resonance image (MRI) disclosed a hyperintense left occipital and posterior temporal lesion (Fig 1A). At 17 years, the patient suffered from sudden and permanent visual loss (visual acuity 1/10 bilaterally). Neurological examination

showed bilateral hearing loss, alexia without agraphia, constructional apraxia, memory loss, bilateral optic atrophy, and a mild pyramidal syndrome on the left side. He then developed intention tremor of right upper limb and myoclonic jerks on the left side of the face. Lactate concentrations in blood and cerebrospinal fluid (CSF) were normal. A brain MRI showed improvement of the previously observed lesion; small areas of abnormal signal intensity were noticed in the right temporal lobe, right thalamus, and periaqueductal gray matter (Fig 1B). Two muscle biopsies, taken at 17 and 24 years, were morphologically normal.

### Patient 2

At age 17 years this girl experienced daily episodes of transitory tingling paresthesias involving her left hand and arm. Brain MRI disclosed a hyperintense lesion in the right occipital lobe. Six months later, she reported myoclonic jerks involving the right side of the face. At age 18 years, sudden permanent visual loss (visual acuity 1/10 bilaterally) was accompanied by repeated episodes of throbbing headache, and transitory prickling paresthesias and weakness of the upper left arm. Lactate was normal in blood but increased in the CSF (2818 μM; normal values 800 to 2100). MRI scan disclosed several cortico-subcortical areas of increased signal intensity in

the cerebral hemispheres (Fig 1C) and symmetrical hyperintensities in the posterior basal ganglia (Fig 1D); the previously observed occipital lesion was not found. A muscle biopsy was morphologically normal.

### Patient 3

This 47-year-old male patient was affected by febrile convulsions up to the age of 6 years. At 36 years he noted bilateral hearing loss and, 2 years later, difficulties in walking and sudden, bilateral visual loss (visual acuity 2/10 bilaterally). Neurological examination showed pes cavus, optic atrophy, nasal voice, ataxia of the four limbs, mild distal muscle atrophy, brisk tendon reflexes, and a left Babinski sign. Lactate concentration was normal in blood but slightly increased in CSF (2277  $\mu$ M). Brain MRI showed signs of diffuse supra- and infratentorial atrophy (not shown). A muscle biopsy disclosed several ragged-red fibers.

Family histories from the three patients were all negative for neurological disorders and visual loss. All three patients were unrelated, as demonstrated by the presence of several different polymorphisms detected in the D-loop region of their mtDNA (not shown). In all three patients the visual loss was associated with optic atrophy, resembling Leber's hereditary optic neurodegeneration (LHON); however, the transient peripapillary vessel proliferation typically seen in LHON could not be documented because the patients were examined after the acute onset of visual loss.

## Methods

### Morphological and Biochemical Analyses

Morphological analysis of skeletal muscle and biochemical assays of the individual respiratory complexes on muscle homogenate were carried out as described.<sup>6</sup> Specific activities of each complex were normalized to that of citrate synthase (CS), an indicator of the number of mitochondria.

### Silver-Staining Single-Stranded Conformation

#### Polymorphism and Sequencing Analysis

The 170-base pair (bp) ND5 gene region from nucleotide position (np) 13,430 to 13,600 of mtDNA<sup>7</sup> was polymerase chain reaction (PCR)-amplified from total DNA using standard procedures. Single-stranded conformation polymorphism (SSCP) and DNA sequence analysis were performed as described.<sup>6</sup>

### HaeIII and BglII Restriction Fragment Length Polymorphism Analysis

The 13514A→G transition creates an HaeIII-specific restriction site which was used for restriction fragment length polymorphism (RFLP) analysis on a 125-bp PCR fragment encompassing np 13,430 to 13,555 of mtDNA.<sup>7</sup> In the presence of the mutation, the fragment was cleaved into 84- and 41-bp fragments. RFLP analysis of the 13513G→A transition was performed as described.<sup>8</sup> The cleaved fragments were separated from the corresponding uncut fragments by agarose-gel electrophoresis. The proportion of mutant versus total mtDNA was calculated by densitometry.

### Cybrids

Transmitochondrial cybrids were obtained by polyethylene glycol fusion of fibroblast-derived cytoplasts from Patient 2 and a 143B rho-zero cell line, as previously described.<sup>9</sup> After selection, six clones with variable amounts of 13514G mutant mtDNA were obtained, together with numerous clones containing only 13514A wild-type mtDNA.

## Results and Discussion

Biochemical assay performed on muscle homogenates showed a partial reduction of the complex I/CS ratio (Table I). Moreover, the most common pathogenic mutations of mtDNA were absent in the three patients (see the Mitomap Web site: <http://www.gen.emory.edu/mitomap.html>). These findings and the recent report of the 13513G→A mutation in MELAS subjects prompted us to analyze the critical region of the ND5 gene. As shown in Figure 2A, a similar SSCP pattern was present in samples from Patients 1 and 2, whereas a different pattern was obtained in Patient 3. Nucleotide sequence analysis showed the presence of the 13513G→A mutation in Patient 3 (not shown), whereas in both Patients 1 and 2 an identical 13514A→G transition was detected (Fig 2B). Both mutations were heteroplasmic and affected the same amino acid residue in the ND5 subunit. However, the 13513G→A mutation led to a D393N amino acid change, whereas the 13514A→G mutation caused a D393G change. In Patient 1, the 13514A→G mutation was much more abundant in the two muscle biopsies (70%) than in fibroblast (12%) or blood (4%) mtDNA. No mutation was de-

Table. Biochemical Activities in Muscle Homogenate

|                                       | Complex I/CS | Complex II/CS | Complex III/CS | Complex IV/CS | CS           |
|---------------------------------------|--------------|---------------|----------------|---------------|--------------|
| Patient 1 <sup>a</sup>                | 9.6          | 22.8          | 98             | 109           | 219          |
| Patient 2                             | 10.4         | 26.2          | 173            | 106           | 146          |
| Patient 3                             | 15.2         | ND            | 146            | 96            | 152          |
| Controls <sup>b</sup> (mean $\pm$ SD) | 24 $\pm$ 4   | 30.0 $\pm$ 5  | 120 $\pm$ 20   | 90 $\pm$ 14   | 160 $\pm$ 30 |

<sup>a</sup>Values are from the second biopsy.

<sup>b</sup>n = 30.

CS = citrate synthase; ND = not done.

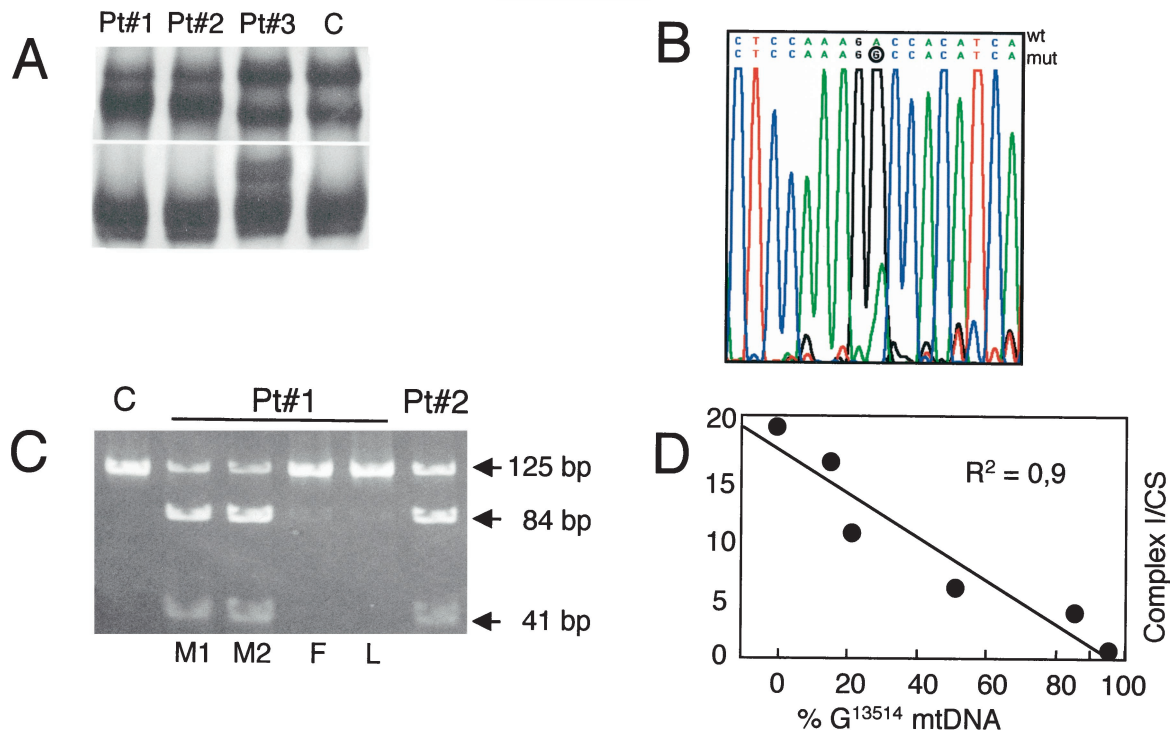


Fig 2. Identification of the 13514A→G mutation. (A) Single-stranded conformation polymorphism analysis of a polymerase chain reaction fragment encompassing muscle mtDNA from np 13,430 to 13,600. Two areas of the same gel are shown: The top area contains single-stranded DNA; the bottom area contains heteroduplex species. In the single-stranded DNA area, the samples from Patients 1 and 2 give an identical pattern which differs from that of a control sample (C). In the heteroduplex zone (bottom), an aberrant band is present in the sample from Patient 3. (B) Nucleotide sequence analysis of mtDNA extracted from muscle of Patient 1. A smaller peak corresponding to wild-type (wt) A is visible under a major peak corresponding to the mutant (mut) G (encircled). (C) HaeIII- restriction fragment length polymorphism analysis of several DNA samples of Patient 1 (M1 = first muscle biopsy; M2 = second muscle biopsy; F = fibroblasts; L = lymphocytes) and from muscle DNA samples of Patient 2 and a control (C). (D) Scattergram and linear regression between the proportion of G13514 mutant mtDNA and the respiratory chain complex I activity normalized to cytrate synthase, in 143B-derived cybrid clones.  $R^2$  is the coefficient of correlation.

tected in blood mtDNA from the patient's mother and three siblings (not shown). Approximately 55% mutant mtDNA was detected in muscle of Patient 2 (Fig 2C) and Patient 3 (not shown). 143B-derived cybrids containing different proportions of mutant mtDNA were obtained from fibroblasts of Patient 2. As shown in Figure 2D, the relative amount of mutant mtDNA was linearly correlated with reduction of complex I/CS ratio in several cybrid clones ( $R^2 = 0.9$ ). This result cannot result from variable repopulation of mtDNA in different cybrid clones because the complex IV/CS ratio was normal in all of them (not shown). The strong correlation found between 13514A→G heteroplasmy and defective complex I activity in cybrids indicates the pathogenic role of this mutation.

After the first report by Santorelli et al,<sup>10</sup> the 13513G→A mutation has been found in four additional individuals, one affected by an MELAS/LHON overlap syndrome and three by typical MELAS.<sup>8</sup>

Our Case 3 confirms that this mutation can cause a mitochondrial encephalomyopathy. However, the clin-

ical presentation was different from classical MELAS. No strokelike episodes were recorded clinically or neuroradiologically; the clinical picture was dominated by the severe visual loss owing to optic atrophy and by a progressive neurological syndrome mainly affecting the motor system.

The 13514A→G is a novel mutation found in two unrelated MELAS-like patients. The MRI findings clearly demonstrated the presence of lesions that predominantly affected gray matter with some adjacent white-matter involvement, as typically seen in MELAS.<sup>11</sup> The mutation was absent in more than 100 control DNA samples from Italians. In both patients muscle morphology was normal, confirming that absence of overt structural abnormalities does not exclude the presence of a mitochondrial disorder.

The discovery in several unrelated patients of two heteroplasmic mutations affecting the same amino acid residue conclusively establishes their pathogenicity and demonstrates that the D393 is indeed crucial for the function of ND5 and complex I.

Similar to the recent report by Pulkes et al,<sup>8</sup> in all three of our cases visual loss due to subacute optic atrophy was a major finding suggesting a correlation between severe involvement of the optic nerve and amino acid changes at D393. Search for D393 mutations should be part of the routine screening for MELAS or MELAS/LHON overlap syndromes.

---

This study was supported by Fondazione Telethon-Italy (grant 1181 to MZ), Min. San. ICS 030.3/RF98.37, and an EU grant on "Mitochondrial Biogenesis in Development and Disease."

We are indebted to B. Geehan for revising the manuscript.

---

## References

1. Goto Y, Nonaka I, Horai S. A mutation in the tRNA(Leu)(UUR) gene associated with the MELAS subgroup of mitochondrial encephalomyopathies. *Nature* 1990;348:651–653.
2. Ciafaloni E, Ricci E, Shanske S, et al. MELAS: clinical features, biochemistry, and molecular genetics. *Ann Neurol* 1992;31:391–398.
3. Mariotti C, Savarese N, Suomalainen A, et al. Genotype to phenotype correlations in mitochondrial encephalomyopathies associated with the A3243G mutation of mitochondrial DNA. *J Neurol* 1995;242:304–312.
4. Maassen JA, Jansen JJ, Kadowaki T, et al. The molecular basis and clinical characteristics of Maternally Inherited Diabetes and Deafness (MIDD), a recently recognized diabetic subtype. *Exp Clin Endocrinol Diabetes* 1996;104:205–211.
5. Damian MS, Seibel P, Reichmann H, et al. Clinical spectrum of the MELAS mutation in a large pedigree. *Acta Neurol Scand* 1995;92:409–415.
6. Tiranti V, Carrara F, Confalonieri P, et al. A novel mutation (8342G→A) in the mitochondrial tRNA(Lys) gene associated with progressive external ophthalmoplegia and myoclonus. *Neuromuscul Disord* 1999;9:66–71.
7. Anderson S, Bankier AT, Barrell BG, et al. Sequence and organization of the human mitochondrial genome. *Nature* 1981;290:457–465.
8. Pulkes T, Eunson L, Patterson V, et al. The mitochondrial DNA G13513A transition in ND5 is associated with a LHON/MELAS overlap syndrome and may be a frequent cause of MELAS. *Ann Neurol* 1999;46:916–919.
9. King M, Attardi G. Human cells lacking mitochondrial DNA: repopulation with exogenous mitochondria by complementation. *Science* 1989;246:500–503.
10. Santorelli FM, Tanji K, Kulikova R, et al. Identification of a novel mutation in the mtDNA ND5 gene associated with MELAS. *Biochem Biophys Res Commun* 1997;238:326–328.
11. Koo B, Becker LE, Chuang S, et al. Mitochondrial encephalomyopathy, lactic acidosis, stroke-like episodes (MELAS): clinical, radiological, pathological, and genetic observations. *Ann Neurol* 1993;34:25–32.

# Decreased Binding of [<sup>11</sup>C]Flumazenil in Angelman Syndrome Patients with GABA<sub>A</sub> Receptor β<sub>3</sub> Subunit Deletions

Irma E. Holopainen, MD, PhD,<sup>1,2</sup>  
E.-Liisa Metsähonkala, MD,<sup>2</sup> Hannaleena Kokkonen, MD,<sup>5</sup>  
Riitta K. Parkkola, MD,<sup>3</sup> Tuula E. Manner, MD,<sup>4</sup>  
Kjell Nägren, PhD,<sup>6</sup> and Esa R. Korpi, MD, PhD<sup>1</sup>

---

**We used positron emission tomography (PET) to study brain [<sup>11</sup>C]flumazenil (FMZ) binding in four Angelman syndrome (AS) patients. Patients 1 to 3 had a maternal deletion of 15q11-q13 leading to the loss of β<sub>3</sub> subunit of γ-aminobutyric acid<sub>A</sub>/benzodiazepine (GABA<sub>A</sub>/BZ) receptor, whereas Patient 4 had a mutation in the ubiquitin protein ligase (UBE3A) saving the β<sub>3</sub> subunit gene. [<sup>11</sup>C]FMZ binding potential in the frontal, parietal, hippocampal, and cerebellar regions was significantly lower in Patients 1 to 3 than in Patient 4. We propose that the 15q11-q13 deletion leads to a reduced number of GABA<sub>A</sub>/BZ receptors, which could partly explain the neurological deficits of the AS patients.**

*Ann Neurol* 2001;49:110–113

---

Angelman syndrome (AS) is a rare neurodevelopmental disorder characterized by severe mental retardation, epilepsy, and delayed motor development.<sup>1</sup> The majority of patients (approximately 70%) have de novo deletions of maternal chromosome 15q11-q13, another 5% to 10% result from uniparental paternal disomy or imprinting mutations, and 4% to 5% of AS patients have a mutation in the E6-AP ubiquitin protein ligase (UBE3A) gene,<sup>1</sup> which is involved in intracellular protein degradation and processing.<sup>2</sup> The exact mechanisms by which the above genetic changes lead to the clinical manifestations of AS remain unclear. In the re-

---

From the <sup>1</sup>Department of Pharmacology and Clinical Pharmacology, University of Turku; Departments of <sup>2</sup>Pediatric Neurology, <sup>3</sup>Diagnostic Radiology, and <sup>4</sup>Anesthesia, University Hospital of Turku, Turku; <sup>5</sup>Department of Clinical Genetics, University Hospital of Oulu, Oulu, and <sup>6</sup>the Turku PET Centre, Turku, Finland.

Received Jan 11, 2000, and in revised form Aug 14. Accepted for publication Aug 17, 2000.

Address correspondence to Dr Holopainen, Department of Pharmacology and Clinical Pharmacology, University of Turku, Kiinamylynkatu 10, FIN-20520 Turku, Finland. E-mail: irma.holopainen@utu.fi

Table 1. Clinical Characteristics, Magnetic Resonance Imaging (MRI), and Molecular Genetic Findings of Patients with Angelman Syndrome

| Patient/Sex | Age (years) | Epilepsy/Seizure Frequency | AED      | MRI                   | Molecular Defect       |
|-------------|-------------|----------------------------|----------|-----------------------|------------------------|
| 1/M         | 2           | No                         | No       | Normal                | Del                    |
| 2/F         | 3           | PGS/1                      | VPA, VGB | Abnormal <sup>a</sup> | Del                    |
| 3/M         | 6           | PGS/3                      | VPA      | Abnormal <sup>a</sup> | Del                    |
| 4/F         | 19          | PGS/4                      | VPA      | Normal                | Mutation in UBE3A gene |

<sup>a</sup>Patients had abnormally small pons and cerebellar vermis.

AED = antiepileptic drug; VGB = vigabatrin; VPA = sodium valproate; Del = maternal deletion of 15q11–q13 including GABRB3; PGS = partial secondarily generalized epilepsy; M = male; F = female. Seizure frequency is given as seizures during the past year.

maining 10% to 15% of AS cases no genetic defects have yet been detected.

Gamma-aminobutyric acid (GABA) is the principal inhibitory neurotransmitter in the central nervous system. It exerts rapid effects through GABA<sub>A</sub> receptors, which are multisubunit complexes and exist as several pharmacologically different subtypes.<sup>3</sup> The genes encoding  $\beta 3$ ,  $\alpha 5$ , and  $\gamma 3$  subunits map to human chromosome 15q11–q13 within the imprinted AS deletion region.<sup>4,5</sup> A recent *gabbr3* knockout mouse line<sup>6</sup> has a high early postnatal mortality, but the survivors have epilepsy and a phenotype with marked similarities to AS patients,<sup>5</sup> suggesting that the GABRB3 gene in humans could contribute to the clinical manifestations of AS. Furthermore, the  $\beta 3$  knockout mice have reduced brain GABA<sub>A</sub> receptor levels.<sup>6</sup>

[<sup>11</sup>C]Flumazenil (FMZ) is a benzodiazepine site (BZ) antagonist with high affinity for brain GABA<sub>A</sub> receptors and is used in positron emission tomography (PET) as a selective ligand to detect GABA<sub>A</sub> receptors.<sup>7</sup> Using this methodology, we studied whether AS patients with maternal 15q11–q13 deletion would have lower [<sup>11</sup>C]FMZ binding than an AS patient with the mutation in the UBE3A gene, which is not known to affect the transcription of GABA<sub>A</sub> receptor subunits.

## Patients and Methods

### Patients and Genetic Analysis

Four patients (2 girls and 2 boys), aged 2 to 19 years, participated in the study (Table 1). Genomic DNA of the patients and their parents was extracted by standard methods. Restriction fragment length polymorphism, quantitative and/or microsatellite analysis, and methylation test were done as earlier described<sup>8</sup> using additional markers in methylation ( $\alpha$ -SNRPN,<sup>9</sup>) and microsatellite (D15S11, D15S122, D15S128, D15S156) analysis. Screening for UBE3A mutation by conformation-sensitive gel electrophoresis and sequencing were carried out as described by Rapakko et al (unpublished data).

### [<sup>11</sup>C]Flumazenil Positron Emission Tomography and Magnetic Resonance Imaging

The positron emission tomography (PET) examinations were done at the Turku PET Centre, Turku, Finland, with

[<sup>11</sup>C]flumazenil, [<sup>11</sup>C]FMZ, using a 12-ring PET scanner (Advance General Electric Medical Systems, Milwaukee, WI). [<sup>11</sup>C]FMZ was synthesized using [<sup>11</sup>C]-methyl triflate as a precursor.<sup>10</sup> Radiochemical purity of <sup>11</sup>C was over 99.5%. The injected dose was 3.7 MBq/kg and the specific activity at the time of injection  $24.3 \pm 6.5$  GBq/ $\mu$ mol (micro) (mean  $\pm$  standard error of the mean [SEM]) with an injected mass of  $1.62 \pm 0.85$   $\mu$ g of flumazenil. The dynamic scan lasted 60 minutes. All PET studies were performed under propofol anesthesia (3 to 8 mg/kg body weight/hr). None of the patients received premedication. For the calculation, individually shaped regions of interest were drawn on two planes on the frontal, occipital, parietal, hippocampal, cerebellar, and pontal areas with the help of corresponding resliced magnetic resonance imaging (MRI) images (1.5 T; Siemens Somatom<sup>®</sup> SP 63, Erlangen, Germany) (LM). The results are given as binding potential (BP) ( $B_{\max}/K_d$ ) according to Hume et al,<sup>11</sup> describing the ratio of the maximal number of binding sites multiplied by their affinity for the ligand. The pons was used as a reference area.

### Statistical Analysis of the [<sup>11</sup>C]FMZ Binding Data

The significance of differences in BP among the different brain areas in Patients 1 to 3 as a group was analyzed with repeated analysis of variance, and separately in each patient with Tukey–Kramer multiple comparison test, with the level of significance set at  $p < 0.05$ . The significance of differences between Patients 1 to 3 and Patient 4 was as

Table 2. [<sup>11</sup>C]Flumazenil Binding Potentials in Patients with Angelman Syndrome

| Brain Area       | Patients 1 to 3 |               | Patient 4        |                  |
|------------------|-----------------|---------------|------------------|------------------|
|                  | Right           | Left          | Right            | Left             |
| Frontal cortex   | 3.0 $\pm$ 0.7   | 2.9 $\pm$ 0.8 | 4.6 <sup>a</sup> | 4.7 <sup>a</sup> |
| Occipital cortex | 3.6 $\pm$ 0.7   | 3.7 $\pm$ 0.7 | 4.0              | 4.3              |
| Parietal cortex  | 3.1 $\pm$ 0.7   | 2.9 $\pm$ 0.6 | 4.5 <sup>a</sup> | 4.3 <sup>a</sup> |
| Hippocampus      | 2.5 $\pm$ 0.3   | 2.7 $\pm$ 0.3 | 3.2 <sup>a</sup> | 3.3 <sup>a</sup> |
| Cerebellum       | 2.1 $\pm$ 0.4   | 2.1 $\pm$ 0.5 | 3.6 <sup>a</sup> | 3.2 <sup>a</sup> |

The results for Patients 1 to 3 are given as means  $\pm$  standard deviation. The binding potential values of Patients 1 to 3 differed significantly ( $p < 0.0001$ ) between various brain regions (repeated analysis of variance).

<sup>a</sup>Value is significantly ( $p < 0.05$ ) different from the corresponding values of Patients 1 to 3 (Student's independent two-tailed  $t$  test).

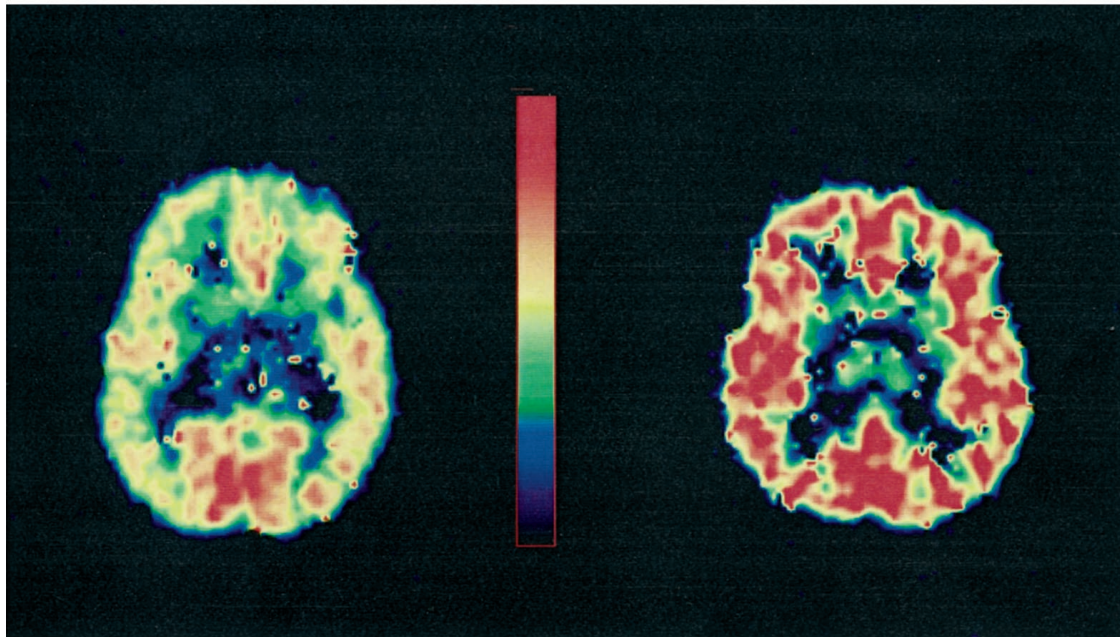


Fig. Pixel-by-pixel images of [<sup>11</sup>C]flumazenil binding potential in Patient 3 with the maternal 15q11-q13 deletion (at the left) and in Patient 4 with the UBE3A mutation (at the right). The PET images illustrate the binding potential at the corresponding low fronto-temporo-occipital level in both patients.

essed with the Student's independent two-tailed *t* test, the level of significance being set at  $p < 0.05$ .

#### Ethics

Informed consent was obtained from the parents (all patients were severely mentally retarded) for the [<sup>11</sup>C]FMZ-PET studies. The study was approved by the Joint Ethics Committee of the Medical Faculty of the University of Turku and the University Hospital of Turku.

#### Results

Table 1 gives the clinical characteristics of the AS patients and their main MRI and molecular genetic findings. Patients 1 and 3 had a common large maternal deletion in chromosome 15q11-q13 covering the loci from D15S9 to D15S12/D15S156, which included a deletion of subunits  $\beta 3$ ,  $\alpha 5$ ,  $\gamma 3$ . Patient 2 had a maternal deletion at least from loci D15S11 to D15S97, including the deletion of subunit  $\beta 3$  gene. Patient 4 had a frameshift mutation in the UBE3A gene due to 2 bp deletion in exon 9. Table 2 gives the results of [<sup>11</sup>C]FMZ BP values. The BP values of Patients 1 to 4 did not differ significantly between the right and left side in any brain area. In Patient 1, the BP in the cerebellar region was significantly lower ( $p < 0.05$ ) than in any other brain region, and in Patients 2 to 4 the BP in the hippocampal and cerebellar regions was significantly lower ( $p < 0.05$ ) than in the other brain regions. The BP values of Patients 1 to 3 were significantly lower ( $p < 0.05$ ) than those of Patient 4 in all brain regions studied other than the occipital area. The

Figure shows the [<sup>11</sup>C]FMZ-PET images of Patients 3 and 4.

#### Discussion

The main finding of this study was the significantly lower [<sup>11</sup>C]FMZ binding in the frontal, parietal, hippocampal, and cerebellar areas of the AS patients with 15q11-q13 deletion than in those of an AS patient with UBE3A mutation. To our knowledge, this is the first report in which the [<sup>11</sup>C]FMZ-PET method is used to study the possible role of GABA<sub>A</sub>/BZ receptors in AS. Our finding is in keeping with a recent iodine-123 iomazenil single-photon emission tomography (SPECT) study, in which an adult AS patient with 15q11-q13 deletion had cerebellar atrophy as well as a severely decreased density of BZ receptors in the cerebellum and a mildly decreased density in the frontal and temporal cortices.<sup>12</sup>

[<sup>11</sup>C]FMZ binds to GABA<sub>A</sub>/BZ receptors with high specificity and reliably detects focal changes in the GABA<sub>A</sub>/BZ receptors in humans.<sup>7</sup> The influence of anesthesia, age, and antiepileptic medication on [<sup>11</sup>C]FMZ binding can be considered only indirectly. The PET study was performed under propofol anesthesia on all patients, so the effect of anesthesia was the same for all patients. The binding of flumazenil may decrease with age in some brain regions as shown in animals,<sup>13</sup> whereas valproate treatment may reduce the number of GABA<sub>A</sub>/BZ receptors,<sup>14</sup> factors which fail to directly explain our findings. The seizure frequency

of Patients 2 to 4 was low, and Patient 1 had no epilepsy; thus, epilepsy itself cannot explain the differences in [ $^{11}\text{C}$ ]FMZ BP between the patient groups. Thus, we propose that the lower [ $^{11}\text{C}$ ]FMZ BP in Patients 1 to 3 was due to the deletion of  $\beta 3$  subunit, which leads to (1) a reduction in the number of GABA $_A$  receptors, and/or (2) changes in the affinity of remaining GABA $_A$ /BZ receptor subtypes. Both of these mechanisms are feasible, but because the  $\beta$  subunits do not affect the affinity of benzodiazepine sites,<sup>15</sup> the second alternative is unlikely. This interpretation is also in line with the finding of remarkably reduced GABA $_A$  receptor density in the whole brains, cerebral cortices, and hippocampi of  $\beta 3$  subunit knockout mice.<sup>6</sup>

Among the patients, [ $^{11}\text{C}$ ]FMZ BP varied between the brain regions, and between the patient groups. Patients 1 to 3 failed to show significantly lower [ $^{11}\text{C}$ ]FMZ BP in the occipital region. This is consistent with preclinical data indicating that the amounts of various pharmacological GABA $_A$  receptor subtypes vary regionally and that the subunit combination determines the ligand binding properties.<sup>3</sup>

Although the contribution of various molecular defects to the pathogenesis of AS is not known, theoretically the UBE3A mutations could disturb axonal growth and neuronal connectivity during development.<sup>2</sup> GABA, by acting via GABA $_A$  receptors, is known to affect brain development.<sup>16</sup> Furthermore, GABA $_A$  receptor  $\beta 3$ ,  $\alpha 5$ , and  $\gamma 3$  subunits are widely expressed in the developing mammalian brain.<sup>17</sup> Therefore, both genetic defects might cause drastic changes at the embryonic and neonatal phase in AS patients, leading to neurodevelopmental defects and clinical AS phenotypes. Low levels of GABA $_A$  receptors could also be a contributing factor in the majority of AS patients.

---

This study was financially supported by the Arvo and Lea Ylppö Foundation to I.E.H. and from the Academy of Finland to E.R.K.

We thank Drs Marck Lalande, Bernhard Horsthemke, Daniel Driscoll, and Uta Francke for kindly providing us with the probes, and Dr Wadelius for the microsatellites D15S113, D15S97, and D15S156.

---

## References

1. Moncla A, Malzac P, Voelckel M-A, et al. Phenotype-genotype correlation in 20 deletion and 20 non-deletion Angelman syndrome patients. *Eur J Hum Genet* 1999;7:131–139.
2. Oh CE, McMahon R, Benzer S, et al. *bendless*, a *Drosophila* gene affecting neuronal connectivity, encodes a ubiquitin-conjugating enzyme homolog. *J Neurosci* 1994;14:3166–3179.
3. Lüddens H, Korpi ER, Seeburg PH. GABA $_A$ /benzodiazepine receptor heterogeneity: neurophysiological implications. *Neuropharmacology* 1995;34:245–254.
4. Glatt K, Glatt H, Lalande M. Structure and organization of GABRB3 and GABRA5. *Genomics* 1997;41:63–69.
5. DeLorey TM, Handforth A, Anagnostaras SG, et al. Mice lacking the  $\beta 3$  subunit of the GABA $_A$  receptor have the epilepsy phenotype and many of the behavioral characteristics of Angelman syndrome. *J Neurosci* 1998;18:8505–8514.
6. Homanics GE, DeLorey TM, Firestone LL, et al. Mice devoid of  $\gamma$ -aminobutyrate type A receptor  $\beta 3$ -subunit have epilepsy, cleft palate, and hypersensitive behavior. *Proc Natl Acad Sci USA* 1997;94:4143–4148.
7. Koeppe MJ, Hand KSP, Labbé C, et al. In vivo [ $^{11}\text{C}$ ]flumazenil-PET correlates with ex vivo [ $^3\text{H}$ ]flumazenil autoradiography in hippocampal sclerosis. *Ann Neurol* 1998;43:618–626.
8. Kokkonen H, Kähkönen M, Leisti J. A molecular and cytogenetic study in Finnish Prader-Willi patients. *Hum Genet* 1995;95:568–571.
9. Glenn CC, Nicholls RD, Robinson WP, et al. Modification of 15q11–q13 DNA methylation imprints in unique Angelman and Prader-Willi patients. *Hum Mol Genet* 1993;2:1377–1382.
10. Nägren K, Halldin C. Methylation of amide and thiol functions with [ $^{11}\text{C}$ ]methyltriflate, as exemplified by [ $^{11}\text{C}$ ]NMSP, [ $^{11}\text{C}$ ]flumazenil and [ $^{11}\text{C}$ ]methionine. *J Label Comp Rad* 1998;41:831–841.
11. Hume SP, Myers R, Bloomfield PM, et al. Quantitation of carbon-11-labeled raclopride in rat striatum using positron emission tomography. *Synapse* 1992;12:47–54.
12. Odano I, Anezaki T, Ohkubo M, et al. Decrease in benzodiazepine receptor binding in a patient with Angelman syndrome detected by iodine-123 iomazenil and single-photon emission tomography. *Eur J Nucl Med* 1996;23:598–604.
13. Pratt GD, Richter A, Möhler H, et al. Regionally selective and age-dependent alterations in benzodiazepine receptor binding in the genetically dystonic hamster. *J Neurochem* 1995;64:2153–2158.
14. Pevett MC, Lammertsma AA, Brooks DJ, et al. Benzodiazepine-GABA $_A$  receptors in idiopathic generalized epilepsy measured with [ $^{11}\text{C}$ ]flumazenil and positron emission tomography. *Epilepsia* 1995;36:113–121.
15. Lüddens H, Korpi ER. GABA antagonists differentiate between recombinant GABA $_A$ /benzodiazepine receptor subtypes. *J Neurosci* 1995;15:6957–6962.
16. Ben-Ari Y, Khazipov R, Leinekugel X, et al. GABA $_A$ , NMDA and AMPA receptors: a developmentally regulated “ménage à trois.” *Trends Neurosci* 1997;20:523–529.
17. Laurie DJ, Wisden W, Seeburg PH. The distribution of thirteen GABA $_A$  receptor subunit mRNAs in the rat brain. III. Embryonic and postnatal development. *J Neurosci* 1992;12:4151–4172.

# No Evidence for Genetic Association or Linkage of the Cathepsin D (*CTSD*) Exon 2 Polymorphism and Alzheimer Disease

Lars Bertram, MD,<sup>1</sup> Suzanne Guénette, PhD,<sup>1</sup> Jennifer Jones, BS,<sup>1</sup> Devon Keeney, MS,<sup>1</sup> Kristina Mullin, BS,<sup>1</sup> Adam Crystal, BA,<sup>2</sup> Sanjay Basu,<sup>1</sup> Stephen Yhu, BS,<sup>1</sup> Amy Deng, PhD,<sup>2</sup> G. William Rebeck, PhD,<sup>2</sup> Bradley T. Hyman, MD, PhD,<sup>2</sup> Rodney Go, PhD,<sup>3</sup> Melvin McInnis, MD,<sup>4</sup> Deborah Blacker, MD, ScD,<sup>5,6</sup> and Rudolph Tanzi, PhD<sup>1</sup>

**Two recent case-control studies have suggested a strong association of a missense polymorphism in exon 2 of the cathepsin D gene (*CTSD*) and Alzheimer disease (AD). However, these findings were not confirmed in another independent study. We analyzed this polymorphism in two large and independent AD study populations and did not detect an association between *CTSD* and AD. The first sample was family-based and included 436 subjects from 134 sibships discordant for AD that were analyzed using the sibship disequilibrium test (SDT,  $p = 0.68$ ) and the sib transmission/disequilibrium test (Sib-TDT,  $p = 0.81$ ). The second sample of 200 AD cases and 182 cognitively normal controls also failed to show significant differences in the allele or genotype distribution in cases versus controls ( $X^2$ ,  $p = 0.91$  and  $p = 0.88$ , respectively). In addition, two-point linkage analyses in an enlarged family sample ( $n = 670$ ) did not show evidence for linkage of the chromosomal region around *CTSD*. Thus, our analyses on more than 800 subjects suggest that if an association between the *CTSD* exon 2 polymorphism and AD exists, it is likely to be smaller than previously reported.**

Ann Neurol 2001;49:114–116

Cathepsin D (catD) is a plausible candidate for genetic association with Alzheimer disease (AD), a genetically

From the <sup>1</sup>Genetics and Aging Unit, <sup>2</sup>Department of Neurology, Massachusetts General Hospital, Harvard Medical School, Charlestown, MA; <sup>3</sup>Department of Epidemiology, School of Public Health, University of Alabama, Birmingham, AL; <sup>4</sup>Department of Psychiatry, Johns Hopkins University Medical Institutions, Baltimore, MD; <sup>5</sup>Department of Psychiatry, Massachusetts General Hospital, Harvard Medical School, Charlestown, MA; and the <sup>6</sup>Department of Epidemiology, Harvard School of Public Health, Boston, MA.

Received Jul 10, 2000. Accepted for publication Aug 18, 2000.

Address correspondence to Dr Tanzi, Genetics and Aging Unit, MGH-East, 149 13th Street, Charlestown, MA 02129.  
E-mail: tanzi@helix.mgh.harvard.edu

complex and heterogeneous disorder. As an intracellular acid protease, catD has been implicated in the processing of the amyloid precursor protein (APP) and tau in vitro,<sup>1–3</sup>, i.e., two proteins that are intimately involved in AD neuropathology. A common polymorphism in the coding region of the catD gene (*CTSD*) that results in an amino acid change at residue 224 (Ala→Val) has been associated with increased protein expression.<sup>4</sup> Recently, Papassotiropoulos and colleagues reported the results of two independent case-control studies in which there was a highly significant overrepresentation of the T-allele of this polymorphism in AD patients.<sup>5,6</sup> From these findings, the authors estimated odds ratios of 2.4<sup>5</sup> and 3.1<sup>6</sup> in carriers versus noncarriers of this allele. Furthermore, carriers of both the T-allele for *CTSD* and at least one ε4-allele at the apolipoprotein E locus (*APOE*) were reported to be almost 20 times more likely to have AD than noncarriers of these alleles.<sup>6</sup> Because of the potential importance of these findings, we tested two large and independent samples using family-based as well as case-control methodologies, but saw no evidence for association. Our negative findings are in accordance with another, albeit smaller, case-control study from Northern Ireland.<sup>7</sup>

## Methods

### Patients

Subjects for the family-based analyses were collected as part of the National Institute of Mental Health (NIMH) Genetics Initiative following a standardized protocol applying NINCDS/ADRDA criteria for the diagnosis of AD.<sup>8</sup> These included a total of 670 subjects that were drawn from 270 families. This sample was used for determination of genotype distribution (Table 1), calculation of mean ages of onset in affected subjects (69.8 years, standard deviation [SD] 8.1), and genetic linkage analyses. Approximately two thirds of these subjects ( $n = 436$ , affected  $n = 264$ , unaffected  $n = 172$ ) came from discordant sibships ( $n = 134$ ) and were used in family-based association studies.

Subjects for the case-control sample were collected from the Alzheimer Disease Research Center (ADRC) at Massachusetts General Hospital, following protocols described ear-

Table 1. Genotype Distribution in National Institute of Mental Health Families

| <i>CTSD</i> genotypes | Affected <sup>a</sup><br>(n = 496) | Unaffected <sup>a</sup><br>(n = 174) |
|-----------------------|------------------------------------|--------------------------------------|
| CC                    | 401                                | 146                                  |
| CT                    | 92                                 | 25                                   |
| TT                    | 3                                  | 3                                    |

<sup>a</sup>Allele and genotype frequencies are not independent in family-based samples, both within and across affected and unaffected individuals.

lier.<sup>9</sup> This sample included 200 AD patients (37 of whom had neuropathologically confirmed AD) as well as 182 cognitively normal controls and is comparable in size to the samples used in the original studies.<sup>5,6</sup> Allele and genotype frequencies of this sample are displayed in Table 2. Mean age of onset was 70.8 years (SD 9.3, n = 196) in AD cases; mean age at examination in controls was 66.5 years (SD 11.5).

### Genotyping

*APOE* was genotyped in all subjects as described previously.<sup>10</sup> The exon 2 polymorphism of *CTSD* was genotyped in all subjects using the same polymerase chain reaction conditions as in the original study<sup>5</sup> followed by an overnight digest with *MwoI* and 6% polyacrylamide (NIMH sample) and 4% agarose (ADRC sample) gelelectrophoresis.

### Statistical Techniques

To test for association in the NIMH families, we used two family-based association tests that do not require parental data: the sibship disequilibrium test (SDT)<sup>11</sup> as well as the sib transmission/disequilibrium test (Sib-TDT).<sup>12</sup> The SDT is a nonparametric sign test developed for use with sibling pedigree data that compares the average number of candidate alleles between affected and unaffected siblings in each family.<sup>11</sup> The Sib-TDT is numerically equivalent to the Mantel-Haenszel test of trend<sup>13</sup> and compares the allele distribution in discordant sib-pairs. Like the TDT and other family-based association tests, these methods are not susceptible to bias owing to population admixture. We also performed conditional logistic regression stratified on family, using *CTSD* T-allele and *APOE*  $\epsilon 4$ -allele carrier status to look at any effect of these genes separately and together. To test for linkage in the *CTSD* region, we performed parametric two-point linkage analyses (using FASTLINK) with two autosomal dominant disease models (affected-only and age-dependent penetrance) as described earlier.<sup>14</sup> Linkage analyses were done on the sample as a whole as well as on strata divided by *APOE* genotype, onset age, or both. In the ADRC case-control sample, allele and genotype frequencies were compared by computing  $\chi^2$ -tests in contingency tables. Power analyses using the STATA program determined that the sample size of the case-control study alone was sufficient to detect an association of the magnitude reported<sup>5,6</sup> with a power of over 90%.

Table 2. Allele Frequencies and Genotype Distribution in Alzheimer Disease Research Center Case-Control Sample

|                       | Cases (n = 200) | Controls (n = 182) |
|-----------------------|-----------------|--------------------|
| <i>CTSD</i> genotypes |                 |                    |
| CC                    | 167             | 152                |
| CT                    | 31              | 29                 |
| TT                    | 2               | 1                  |
| Allele frequencies    |                 |                    |
| C                     | 0.913           | 0.915              |
| T                     | 0.087           | 0.085              |

## Results

Neither the SDT nor the Sib-TDT showed evidence of association between the *CTSD* exon 2 polymorphism and AD in discordant sibships of the NIMH data set ( $Z = 0.17$ ,  $p = 0.68$  and  $Z = 0.06$ ,  $p = 0.81$ , respectively). There was no increase in risk for AD in carriers of the *CTSD* T-allele controlling for the presence of *APOE*  $\epsilon 4$ -status in conditional logistic regression (data not shown). Furthermore, there was no evidence of linkage in any of the various strata investigated (maximum LOD scores  $< 1$ , data not shown). Similarly, we could not detect an association between cases and controls in the independent ADRC sample (alleles:  $\chi^2 = 0.013$ ,  $p = 0.91$ , genotypes:  $\chi^2 = 0.26$ ,  $p = 0.88$ ) (Table 2).

## Discussion

Because of the increasing prevalence of AD across many different ethnic groups worldwide, it is critical to identify genetic risk factors in parallel with developing therapeutics that could reduce or inhibit the degree of neurodegeneration caused by this devastating disease. Although there is evidence supporting a biological role of catD in AD neuropathogenesis,<sup>1,3,4</sup> we failed to detect an association of a common polymorphism in the catD gene and AD in two large and carefully ascertained study populations using two different analytic approaches. First, we examined the allele distribution in more than 400 subjects from sibships discordant for the disease using two different family-based association tests, the SDT and the Sib-TDT. The SDT has been validated earlier on the association of AD and the common polymorphism at the *APOE* locus<sup>11</sup> in the NIMH sample. Applied to the dataset of this study, both the overrepresentation of the  $\epsilon 4$  allele of *APOE* as well as the underrepresentation of the  $\epsilon 2$  allele in affected versus unaffected subjects were clearly identified ( $p < 1 \times 10^{-7}$  and  $p = 0.00024$ , respectively, data not shown). Second, we used an identical analytic approach as the original studies<sup>5,6</sup> and tested for association in a case-control sample of comparable size. Again, no evidence for association could be detected between the *CTSD* polymorphism and AD. Finally, performing parametric two-point linkage analyses in all NIMH families, we failed to show evidence for linkage of AD to that chromosomal region across the various strata investigated. These findings are in accordance with the results of a recent whole genome scan in affected sib-pairs of the NIMH sample showing no evidence for linkage of AD to the short arm of chromosome 11,<sup>15</sup> the region where *CTSD* has been mapped (e.g., [http://cedar.genetics.soton.ac.uk/public\\_html/](http://cedar.genetics.soton.ac.uk/public_html/)).

There are several possibilities for how our multiple negative findings can be interpreted in the light of the recently reported and highly significant results. In both analyses, Papasotiropoulos et al applied a case-control

approach to test for association between *CTSD* and AD.<sup>5,6</sup> Despite their good power, these tests are prone to spurious findings owing to population admixture. Although this is less likely to occur if an association is found in two independent study populations—as was done by Papassotiropoulos et al.<sup>6</sup>—it is conceivable that varying allele frequencies for the *CTSD* polymorphism within these populations, eg, owing to subtle ethnic differences, could give rise to the overall significantly different allele distribution in cases versus controls of their study. One possible remedy to protect against the risk of spurious findings due to population admixture is to obtain cases and controls from ethnically homogeneous backgrounds. This was done in the investigation of McIlroy et al, who drew their samples from the relatively homogeneous population in Northern Ireland.<sup>7</sup> However, their study also failed to find a significant association between the *CTSD* polymorphism and AD. A more robust protection against the bias of population admixture is using family-based cases and controls. Several methods have been proposed to test for association in family-based samples, two of which were applied in the present study and both failed to detect a significant effect of the *CTSD* polymorphism and AD. Another issue regarding unverified association results is the possibility of type I errors owing to multiple testing. With many different independent laboratories performing a large number of tests to identify new candidate genes worldwide, it is possible that even replicated findings may be due to type I errors, especially in the light of a bias toward publishing positive results in biomedical journals. It is therefore increasingly important that a postulated positive association between a candidate gene and a disease be replicated (1) across several independent samples (and ideally ethnic groups), while (2) using different analytic approaches to test for association (eg, case-control vs family-based). In AD, only the polymorphism for *APOE* meets these requirements,<sup>16</sup> in contrast to most of the reported associations of other candidate genes, which to date remain unreplicated or at least controversial after subsequent follow-up.

In our investigation testing a common polymorphism in the *catD* gene in two large and independent AD study populations using family-based as well as case-control methodologies, we failed to replicate the highly significant findings recently reported by Papassotiropoulos et al.<sup>5,6</sup> Our results suggest that if an association between this polymorphism and AD exists, it is likely to be smaller than previously suggested.

---

This work was sponsored by grants from the NIMH, NIA (ADRC), and the Alzheimer Association.

LB is a fellow of the Deutsche Forschungsgemeinschaft (DFG).

---

## References

- Cataldo AM, Barnett JL, Pieroni C, et al. Increased neuronal endocytosis and protease delivery to early endosomes in sporadic Alzheimer's disease: neuropathologic evidence for a mechanism of increased beta-amyloidogenesis. *J Neurosci* 1997;17:6142–6151.
- McDermott JR, Gibson AM. Degradation of Alzheimer's beta-amyloid protein by human cathepsin D. *Neuroreport* 1996;7:2163–2166.
- Chevallier N, Vizzavona J, Marambaud P, et al. Cathepsin D displays in vitro beta-secretase-like specificity. *Brain Res* 1997;750:11–19.
- Touitou I, Capony F, Brouillet JP, et al. Missense polymorphism (C/T224) in the human cathepsin D pro-fragment determined by polymerase chain reaction–single strand conformational polymorphism analysis and possible consequences in cancer cells. *Eur J Cancer* 1994;3:390–394.
- Papassotiropoulos A, Bagli M, Feder O, et al. Genetic polymorphism of cathepsin D is strongly associated with the risk for developing sporadic Alzheimer's disease. *Neurosci Lett* 1999;262:171–174.
- Papassotiropoulos A, Bagli M, Kurz A, et al. A genetic variation of cathepsin D is a major risk factor for Alzheimer's disease. *Ann Neurol* 2000;47:399–403.
- McIlroy SP, Dynan KB, McGleenon BM, et al. Cathepsin D gene exon 2 polymorphism and sporadic Alzheimer's disease. *Neurosci Lett* 1999;273:140–141.
- Blacker D, Albert MS, Bassett SS, et al. Reliability and validity of NINCDS-ADRDA criteria for Alzheimer's disease. The National Institute of Mental Health Genetics Initiative. *Arch Neurol* 1994;51:1198–1204.
- Gomez-Isla T, West HL, Rebeck GW, et al. Clinical and pathological correlates of apolipoprotein E epsilon 4 in Alzheimer's disease. *Ann Neurol* 1996;39:62–70.
- Blacker D, Haines JL, Rodes L, et al. ApoE-4 and age at onset of Alzheimer's disease: the NIMH genetics initiative. *Neurology* 1997;48:139–147.
- Horvath S, Laird NM. A discordant-sibship test for disequilibrium and linkage: no need for parental data. *Am J Hum Genet* 1998;63:1886–1897.
- Spielman RS, Ewens WJ. A sibship test for linkage in the presence of association: the sib transmission/disequilibrium test. *Am J Hum Genet* 1998;62:450–458.
- Laird NM, Blacker D, Wilcox M. The sib transmission/disequilibrium test is a Mantel-Haenszel test [letter; comment]. *Am J Hum Genet* 1998;63:1915–1916.
- Blacker D, Wilcox MA, Laird NM, et al. Alpha-2 macroglobulin is genetically associated with Alzheimer disease. *Nat Genet* 1998;19:357–360.
- Keohoe P, Wavrant-De Vrieze F, Crook R, et al. A full genome scan for late onset Alzheimer's disease. *Hum Mol Genet* 1999;8:237–245.
- Farrer LA, Cupples LA, Haines JL, et al. Effects of age, sex, and ethnicity on the association between apolipoprotein E genotype and Alzheimer disease. A meta-analysis. APOE and Alzheimer Disease Meta Analysis Consortium. *JAMA* 1997;278:1349–1356.

# SCA12 Is a Rare Locus for Autosomal Dominant Cerebellar Ataxia: A Study of an Indian Family

Hiroto Fujigasaki, MD, PhD,<sup>1</sup> Ishwar C. Verma, MRCP,<sup>2</sup> Agnès Camuzat, MS,<sup>1</sup> Russell L. Margolis, MD,<sup>4</sup> Cecilia Zander, MS,<sup>1</sup> Anne-Sophie Lebre, MS,<sup>1</sup> Laure Jamot, PhD,<sup>1</sup> Renu Saxena, PhD,<sup>2</sup> Ish Anand MD, DM,<sup>3</sup> Susan E. Holmes, PhD,<sup>4</sup> Christopher A. Ross, MD, PhD,<sup>4,5</sup> Alexandra Dürr, MD, PhD,<sup>1,6,7</sup> and Alexis Brice, MD<sup>1,6,7</sup>

---

**Spinocerebellar ataxia 12 (SCA12) is an autosomal dominant cerebellar ataxia (ADCA) described in a single family with a CAG repeat expansion in the PPP2R2B gene. We screened 247 index cases, including 145 families with ADCA, for this expansion. An expanded repeat ranging from 55 to 61 triplets was detected in 6 affected and 3 unaffected individuals at risk in a single family from India. The association of the PPP2R2B CAG repeat expansion with disease in this new family provides additional evidence that the mutation is causative.**

Ann Neurol 2001;49:117–121

---

At least 12 loci for autosomal dominant cerebellar ataxia (ADCA) are known,<sup>1,2</sup> and five types of ADCAs, designated SCA 1, 2, 3, 6, and 7, are caused by translated CAG repeat expansion in the corresponding gene.<sup>3–9</sup> Recently, Holmes and colleagues reported a single family with a new form of ADCA designated SCA12. The disease was associated with an expanded CAG tract in the 5' untranslated region of the gene encoding PPP2R2B, a brain-specific regulatory subunit of protein phosphatase PP2A, which maps to chromosome 5. Normal repeats ranged from 7 to 28 triplets, whereas expanded repeats ranged from 66 to 78 triplets. However, since this repeat expansion was found in only one family, the expansion might simply have been in linkage disequilibrium with the causative mutation.<sup>10</sup> To

determine the relative frequency and the phenotype associated with the SCA12 expansion, we screened 247 index cases with cerebellar ataxia and found an Indian family in which the disease segregated with the expansion, supporting the hypothesis that this mutation is responsible for the disease. In addition, we show that the distribution of the normal alleles differs significantly in the French and Indian populations.

## Subjects and Methods

### Subjects

Index cases from 145 families with ADCA, 47 with autosomal recessive cerebellar ataxia, and 55 with sporadic progressive cerebellar ataxia were studied. The absence of CAG repeat expansions at the SCA 1, 2, 3, 6, 7, and 8 loci was previously verified. As control subjects, we analyzed 157 French and 100 Indian individuals without neurological disorders. Blood samples were obtained with informed consent, and genomic DNA was extracted using standard methods.

### PCR Analysis of the CAG Repeat Length in the PPP2R2B Gene

A portion of the PPP2R2B gene containing the CAG repeat was amplified by polymerase chain reaction (PCR) with a reaction mixture (25  $\mu$ l) containing 100 ngr genomic DNA, 1  $\mu$ M of each primer,<sup>10</sup> 300  $\mu$ M of each deoxynucleotide triphosphate, 0.2 units Taq DNA polymerase (Perkin-Elmer), and 1% formamide in the buffer provided by the supplier. The cycling steps were 96°C for 3 minutes, 30 cycles of denaturation at 94°C for 45 seconds, annealing at 62°C for 30 seconds, extension at 72°C for 45 seconds, and final extension at 72°C for 7 minutes. The DNA sequences of the PCR products and the number of CAG repeats were determined by automated DNA sequencing and analyses with GeneScan and Genotyper software (PE Applied Biosystems). The lod score was calculated using the software package LINKAGE with the same parameter as previously described.<sup>10</sup>

### Statistical Analysis

The  $\chi^2$  test was used to compare the distributions of all CAG repeat lengths and the frequency of long (>12) and short (<12) triplets in the two populations.

## Results

### Screening for CAG Repeat Expansions in the PPP2R2B Gene in Index Cases

PCR followed by agarose gel electrophoresis showed that only one family out of 145 families with ADCA had an expanded allele (Fig 1a). Expansion at the SCA12 locus was not found in 47 families with autosomal recessive cerebellar ataxia or in the 55 sporadic cases.

### CAG Repeat Analysis in the Indian Family

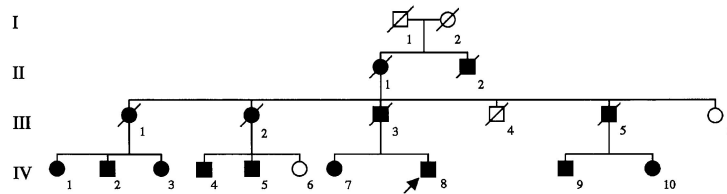
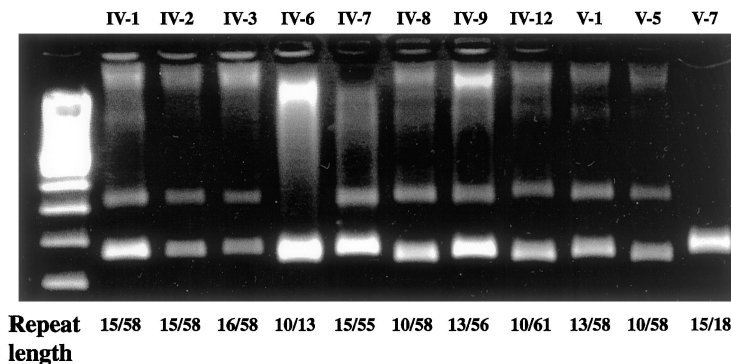
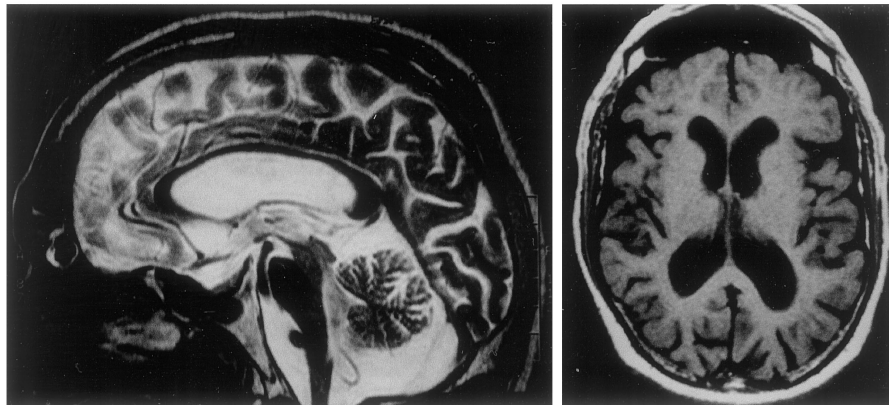
We examined the CAG repeat length in the 11 available members of this family. Nine individuals, 6 af-

---

From <sup>1</sup>INSERM U289, Paris, France; <sup>2</sup>Departments of Medical Genetics and <sup>3</sup>Neurology, Sir Ganga Ram Hospital, New Delhi, India; <sup>4</sup>Division of Neurobiology, Department of Psychiatry, and <sup>5</sup>Department of Neuroscience and the Program in Cellular and Molecular Medicine, Johns Hopkins University School of Medicine, Baltimore, MD; and <sup>6</sup>Fédération de Neurologie and <sup>7</sup>Consultation de Génétique Médicale, Hôpital de la Salpêtrière, Paris, France.

Received May 18, 2000, and in revised form Aug 23. Accepted for publication Aug 23, 2000

Address correspondence to Dr Brice, INSERM U 289, Hôpital de la Salpêtrière, 47, Boulevard de l'Hôpital, 75651 Paris, Cedex 13, France. E-mail: brice@ccr.jussieu.fr

**a****b****c**

*Fig 1. (a) Pedigree of the Indian SCA12 family. The arrow indicates the proband. For reasons of confidentiality, parts of generation IV and generation V are not shown. (b) Polymerase chain reaction (PCR) analysis in the Indian family. PCR products were electrophoresed on 2% agarose gels and visualized with ethidium bromide. Six affected and three asymptomatic at-risk individuals carry expanded alleles. CAG repeat length is indicated at the bottom of the panel. A 100-bp ladder is shown in lane 1. (c) Brain MRI of the SCA12 proband, at age 49, showing atrophy of the cerebellum and the cerebral cortex associated with enlargement of the lateral ventricles. (Left) Sagittal section, T2-weighted image. (Right) Axial section, T1-weighted image.*

affected and 3 asymptomatic at risk, had expanded CAG repeats. The disease cosegregated with the CAG repeat expansion in the family generating a maximal lod score of 1.91 at  $\theta = 0$ . The expansions ranged from 55 to 61 triplets. PCR products amplified from expanded but not from normal alleles contained sequences of different lengths, suggesting mosaicism in blood cells

(data not shown). The CAG repeat was slightly unstable. The allele transmitted maternally to three sibships was not altered, whereas differences of three and five CAG repeats were found in the 2 sibships with paternal transmission (Fig 1b). Three individuals with expansions had no symptoms when sampled at ages 39, 47, and 48.

### *Clinical Features of the Indian Family*

The proband (IV-8), aged 50, developed difficulties in writing and drinking with hand tremor at 40 years of age. He had difficulty in walking at the age of 44. These symptoms have progressed gradually. He has had several episodes of paroxysmal supraventricular tachycardia since the age of 41. On neurological examination at age 41, signs were predominantly of cerebellar involvement. At age 49, he had slurred speech, axial and limb ataxia, and hyperreflexia with bilateral extensor plantar reflex. Ocular examination revealed multipupils in the right eye, broken pursuit, nystagmus on lateral gaze, and slow saccades. There was no weakness, sensory abnormality, or sign of bladder or bowel disturbance. Mental faculties were well maintained, and the proband continued to work as a physician. Brain computed tomographic (CT) scanning and magnetic resonance imaging (MRI) showed cerebellar and cerebral atrophy (Fig 1c). Single-photon emission tomographic (SPECT) analysis revealed reduced uptake of technetium 99m hexamethylpropyleneamine oxin in the cerebellum, the frontal cortex, and the temporal cortex. The electroencephalogram (EEG) and electromyogram (EMG) with nerve conduction studies were normal. Fifteen other family members, including 8 who are still alive, were also affected. Symptoms appeared in almost all affected subjects in their fifth decade and progressed with similar time courses. Subjects IV-1 and IV-2 had memory impairment, including cognitive changes, in addition to severe ataxia when interviewed at ages 65 and 70 (Table).

### *CAG Repeat Analysis in French and Indian Control Subjects*

The distribution of normal PPP2R2B repeat length was determined in 157 French and 100 Indian control subjects. In the French population, normal alleles contained from 9 to 18 CAG triplets, most frequently 10. In the Indian population, lengths of up to 45 triplets were observed. The most common allele in the Indian population also carried 10 triplets. The distribution of the CAG repeat length differed significantly between

the two control populations ( $p < 0.001$ ). The Indian control subjects had a significantly greater proportion of large alleles with more than 12 triplets than did the French ( $p < 0.001$ ; Fig 2). The Indian control subjects with 45 uninterrupted triplets was 28 years old and had no personal or family history of neuropsychiatric disorder.

### **Discussion**

SCA12 is very rare because only 1/247 index cases, only one from India, where the presence of dominant ataxia in most families is not explained by known loci,<sup>11,12</sup> and none of 120 French families with ADCA of unknown cause, carried this mutation.

In this family, the disease cosegregated with the CAG repeat expansion in the PPP2R2B gene in 6 affected subjects. It was also found in 3 unaffected expansion carriers, whose ages ranged from 39 to 48, suggesting the age-dependent penetrance. The size of the expansions, ranging from 55 to 61 triplets, was slightly smaller than in the family previously reported.<sup>10</sup> This is consistent with previous observations that the pathological range of trinucleotide repeat expansions is highly variable<sup>1,13,14</sup> and can only be defined by analyzing large series of patients and control subjects.

The clinical phenotype of the Indian family is relatively homogenous and comparable to that of the initial family.<sup>10</sup> It is particularly interesting that marked cerebral atrophy on MRI was observed in the proband without overt cognitive deficit. The presence of an allele with 45 triplets in a control subject without neurological or psychiatric signs or symptoms and with no family history of ataxia was surprising. This allele, however, was still 10 triplets smaller than those in the affected Indian family and may be like other rare large normal alleles observed in CAG repeat diseases.<sup>1,13,14</sup> Sequence analysis revealed that this allele is not interrupted, as are large normal SCA1 or SCA2 alleles, and mosaicism is clearly visible on an acrylamide gel (data not shown).

The difference in the distributions of normal alleles in the French and Indian populations is striking. The

*Table. Clinical Features of CAG Repeat Carriers in the Indian SCA12 Family*

| Individual | Age (yr) | Age at Onset (yr) | Disease Severity | Dementia | Repeat Length |
|------------|----------|-------------------|------------------|----------|---------------|
| IV-1       | 70       | 40                | +++              | ++       | 15/58         |
| IV-2       | 65       | 40                | ++               | +        | 16/58         |
| IV-3       | 58       | 39                | ++               | —        | 16/58         |
| IV-7       | 56       | 40                | ++               | —        | 15/55         |
| IV-8       | 50       | 41                | +                | —        | 10/58         |
| IV-9       | 51       | 40                | +                | —        | 13/56         |
| IV-12      | 48       | —                 | —                | —        | 10/61         |
| V-1        | 47       | —                 | —                | —        | 13/58         |
| V-5        | 39       | —                 | —                | —        | 10/58         |

Disease severity: — = asymptomatic; + = affected but mild; ++ = walk with support or with great difficulty; +++ = bedridden.

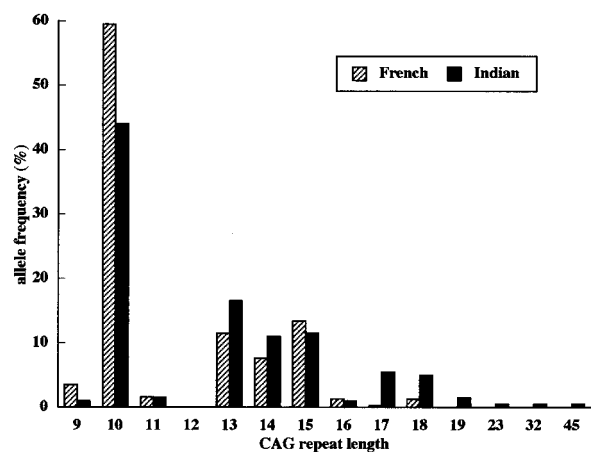


Fig 2. The lengths of SCA12 CAG repeats in French and Indian control populations. The 314 French control chromosomes are represented by hatched bars and the 200 Indian control chromosomes by solid bars. The distributions differ significantly between the two control populations ( $p < 0.001$ ). The number of large alleles with more than 12 triplets was significantly greater in the Indian than in the French control subjects ( $p < 0.001$ ).

greater frequency of large normal alleles in the latter may explain why this new SCA12 family was found in India. It has been known that the relative frequency of various SCAs parallels that of large normal alleles in a given population.<sup>15</sup> Analysis of the distribution of normal alleles and the frequency of SCA12 in different origins would help to confirm this hypothesis.

The mechanism by which the CAG repeat expansion in the PPP2R2B gene causes neurodegeneration remains unknown. The location of the CAG repeat expansion in the 5' region of PPP2R2B, apparently within the 5' UTR, is similar to that of the CGG repeat in FMR1, in which an expansion results in CpG hypermethylation and disruption of transcription, resulting in the fragile X phenotype.<sup>16</sup> It seems plausible that the CAG expansion in PPP2R2B also affects gene expression. In turn, abnormal levels of PPP2R2B may influence the activity of PP2A, leading to the SCA12 phenotype.

In conclusion, we provide several lines of evidence supporting the hypothesis that SCA12 is a causative mutation, not a rare polymorphism in strong linkage disequilibrium with the true mutation: (1) the family has a different geographical origin than the first family described,<sup>10</sup> (2) the expansion cosegregates with the disease, (3) the expansion is at least 10 triplets longer than normal alleles in control subjects from the same population, and (4) the phenotype is similar to that of the original SCA12 kindred. However, additional SCA12 families and studies of control populations are necessary to confirm these observations.

This work was supported by the VERUM Foundation and l'Association Française contre les Myopathies (A.B.) and grants NS 38377 (C.A.R.) and MH01275 (R.L.M.) from the National Institutes of Health. H.F. is supported by a fellowship from the Japan Foundation of Aging and Health. Under a licensing agreement between Johns Hopkins University and Athena Diagnostics, Inc., Drs Holmes, Ross, and Margolis are entitled to a share of royalty received by the university on sales of products (genetic tests) described in this article. The terms of this agreement are being managed by Johns Hopkins University in accordance with its conflict of interest policies.

We thank the proband for his eager assistance in trying to find the cause of his disorder and for enlisting help from the other family members. We thank Drs Christoph B. Lücking, Junko Takahashi, Alexandra Herman, and Patrice Verpillat for their help and Dr Merle Ruberg for critical reading of the manuscript.

## References

- Stevanin G, Dürr A, Brice A. Clinical and molecular advances in autosomal dominant cerebellar ataxias: from genotype to phenotype and pathophysiology. *Eur J Hum Genet* 2000;8:4–18.
- Herman-Bert A, Stevanin G, Netter JC, et al. Mapping of spinocerebellar ataxia 13 to chromosome 19q13.3-q13.4 in a family with autosomal dominant cerebellar ataxia and mental retardation. *Am J Hum Genet* 2000;67:229–35.
- Orr HT, Chung M-Y, Banfi SK, et al. Expansion of an unstable trinucleotide CAG repeat in spinocerebellar ataxia type 1. *Nat Genet* 1993;4:221–226.
- Imbert G, Saudou F, Yvert G, et al. Cloning of the gene for spinocerebellar ataxia 2 reveals a locus with high sensitivity to expanded CAG/glutamine repeats. *Nat Genet* 1996;14:285–291.
- Pulst SM, Nechipork A, Nechipork T, et al. Moderate expansion of a normally biallelic trinucleotide repeat in spinocerebellar ataxia type 2. *Nat Genet* 1996;14:269–276.
- Sanpei K, Takano H, Igarashi S, et al. Identification of the spinocerebellar ataxia type-2 gene using a direct identification of repeat expansion and cloning technique, DIRECT. *Nat Genet* 1996;14:277–284.
- Kawaguchi Y, Okamoto T, Taniwaki M, et al. CAG expansion in novel gene from Machado-Joseph disease at chromosome 14q32.1. *Nat Genet* 1994;8:221–227.
- Zhuchenko O, Bailey J, Bonnen P, et al. Autosomal dominant cerebellar ataxia (SCA6) associated with small polyglutamine expansions in the alpha1A voltage-dependent calcium channel. *Nat Genet* 1997;15:62–69.
- David G, Abbas N, Stevanin G, et al. Cloning of the SCA 7 gene reveals a highly unstable CAG repeat. *Nat Genet* 1997;17:65–70.
- Holmes SE, O'Heam EE, McInnis MG, et al. Expansion of a novel CAG trinucleotide repeat in the 5' region of PPP2R2B is associated with SCA 12. *Nat Genet* 1999;23:391–392.
- Basu P, Chattopadhyay B, Gangopadhyay PK, et al. Analysis of CAG repeats in SCA1, SCA2, SCA3, SCA6, SCA7 and DR-PLA loci in spinocerebellar ataxia patients and distribution of CAG repeats at the SCA1, SCA2 and SCA6 loci in nine ethnic populations of eastern India. *Hum Genet* 2000;106:597–604.
- Saleem Q, Choudhry S, Mukerji M, et al. Molecular analysis of autosomal dominant hereditary ataxias in the Indian population: high frequency of SCA2 and evidence for a common founder mutation. *Hum Genet* 2000;106:179–187.
- Andrew SE, Goldberg YP, Hayden MR. Rethinking genotype and phenotype correlation in polyglutamine expansion disorders. *Hum Mol Genet* 1997;6:2005–2010.

14. Margolis RL, McInnis MG, Rosenblatt A, et al. Trinucleotide repeat expansion and neuropsychiatric disease. *Arch Gen Psychiatry* 1999;56:1019–1031.
15. Takano H, Cancel G, Ikeuchi T, et al. Close association between prevalences of dominantly inherited spinocerebellar ataxia with CAG-repeat expansions and frequencies of large normal CAG alleles in Japanese and Caucasian populations. *Am J Hum Genet* 1998;63:1060–1066.
16. Jin P, Warren ST. Understanding the molecular basis of fragile X syndrome. *Hum Mol Genet* 2000;9:901–908.

## Inherited Myoclonus-Dystonia Syndrome: Narrowing The 7q21-q31 Locus in German Families

Friedrich Asmus, MD,<sup>1</sup> Alexander Zimprich, MD,<sup>1</sup> Markus Naumann, MD,<sup>2</sup> Daniela Berg, MD,<sup>2</sup> Markus Bertram, MD,<sup>3</sup> Andres Ceballos-Baumann, MD,<sup>4</sup> Roswith Pruszk-Seel, MD,<sup>5</sup> Christian Kabus, MD,<sup>6</sup> Martin Dichgans, MD,<sup>1</sup> Sigrid Fuchs, PhD,<sup>7</sup> Bertram Müller-Myhsok, MD,<sup>7</sup> and Thomas Gasser, MD<sup>1</sup>

**Genetic studies were performed in four German families with autosomal dominant myoclonus-dystonia syndrome. Mutations in the D2 dopamine receptor gene, which have been implicated in this disorder, were excluded in all four families by linkage analysis and direct sequencing. All four families supported linkage to the second reported locus on chromosome 7q21 with a combined maximum multipoint lod score of 5.99. The observation of key recombinations in one family refined the disease locus to a 7.2 cM region flanked by the markers D7S652 and D7S2480.**

Ann Neurol 2001;49:121–124

Inherited myoclonus-dystonia syndrome (MDS) is a movement disorder characterized by proximal, bilateral,

From the <sup>1</sup>Neurologische Klinik, Klinikum Großhadern, Ludwig-Maximilians-Universität, München; <sup>2</sup>Neurologische Klinik, Universität Würzburg; <sup>3</sup>Neurologische Klinik, Universität Heidelberg, Heidelberg; <sup>4</sup>Neurologische Klinik, Technische Universität, München; <sup>5</sup>Gesundheitsamt, Norden; <sup>6</sup>Neurologische Klinik, Humboldt Universität, Berlin; and <sup>7</sup>Abteilung für Tropenmedizinische Grundlagenforschung, Bernhard-Nocht Institut für Tropenmedizin, Hamburg, Germany.

The first two authors contributed equally to this work.

Received May 11, 2000, and in revised form Aug 4. Accepted for publication Sep 4, 2000.

Address correspondence to Dr Gasser, Neurologische Klinik, Ludwig-Maximilians-Universität, München Marchioninistrasse 15, D-81377 München, Germany. E-mail: tgasser@nef.med.uni-muenchen.de

myoclonic jerks, usually involving the arms and axial muscles more than legs and gait.<sup>1,2</sup> Typically, myoclonus is responsive to alcohol. Mild dystonia, usually presenting as cervical dystonia and/or writer's cramp in addition to myoclonus, is common but may rarely be the sole symptom of the disease.<sup>3,4</sup> Patients show no other neurological signs or abnormal laboratory findings. In its inherited form, MDS appears to follow an autosomal dominant pattern with reduced penetrance and variable expression.

Recently, two chromosomal loci have been implicated in the disease. One region on chromosome 11q contains the gene for the D2 dopamine receptor and a missense mutation in the third exon (Val154Ile) of this gene was found in one family.<sup>5</sup> Nygaard et al<sup>6</sup> found a chromosomal region spanning 28 cM on chromosome 7q21-q31 to cosegregate with the disease in a single family. In the present study we examined 4 German families with this phenotype. Mutations in the D2 dopamine receptor could be excluded in all families, and the locus on chromosome 7q21 could be confirmed and further narrowed to a 7.2 cM interval.

### Subjects and Methods

#### Patients

This study was approved by the local ethics committee. After giving informed consent, all patients and their relatives were systematically examined by neurologists trained in movement disorders (M.N., D.B., C.K., M.B., T.G.). The diagnosis of MDS was established according to published criteria.<sup>1,2</sup> Venous whole blood samples were taken, and DNA was extracted following standard protocols.

#### Genotype Analysis

We used the following microsatellite markers on chromosomes 7 and 11 spanning the published disease loci: D7S2443 (98.12), D7S820 (104.2), D7S657 (111.37), D7S652 (111.72), D7S476 (112.19), D7S1489 (116.19), D7S1812 (116.19), D7S821 (116.19), D7S2480 (118.92), D7S515 (119.55), D7S796 (120.18), D11S2000 (100.59), DRD2 (104.49), and D11S897 (106.69). The sex-averaged map positions are given in parentheses. They were obtained by calculating the arithmetic mean of the sex-specific distances, taken from The Genetic Location Data Base [http://cedar.genetics.soton.ac.uk/public\_html]. This data base did not include the genetic position of marker D7S515, so the position of the marker was estimated using linear interpolation.

Polymerase chain reaction (PCR) conditions are available from the authors on request. Fluorescent labelled PCR products were analyzed on ABI 310 and ABI 377 (ABI Inc.) automated sequencers with a fluorescence detection system.

#### DNA Sequence Analysis of DRD2

Dideoxy cycle sequencing of PCR products amplified from genomic DNA was performed with the AmpliSequence sequencing kit (Perkin-Elmer, Norwalk, CT) after purification with QUIAquick PCR Purification Kit (Quiagen, Chats-

worth, CA). Primers and PCR conditions for all seven DRD2 exons are available on request.

### Linkage Analysis

Using FASTLINK, VITESSE, and SIMWALK2,<sup>7</sup> we calculated pairwise and multipoint lod scores in all 4 families. Marker allele frequency was assumed to be equal because no reliable population frequencies are available. Only definitely affected individuals were included, to avoid potential problems related to incorrect estimation of penetrance. All other individuals in the pedigrees were considered unknown with respect to disease status. To estimate the maximum lod score obtainable in family I we performed a simulation analysis using SLINK (1,000 replicates, two-point analysis, affecteds-only, marker PIC = 0.87, theta = 0).

## Results

### Phenotypic Description of Pedigrees I–IV

We evaluated 4 families from central Germany, from the coastal area of northern Germany, and from southern Germany. A total of 25 living affecteds (8 women and 17 men) were identified, showing the typical signs of MDS (for pedigrees and summary of clinical characteristics see Fig 1 and the Table). All patients had onset in the first or second decade of life (age range 2–18 years), which is typical of MDS. The disease had a benign and nonprogressive course. Some family

members show true nonpenetrance; they are not affected but have affected offspring (by examination: pedigree III, individuals II:2, III:1, III:3; by family history: pedigree I, individuals I:1, II:1, and pedigree II, individuals III:2, IV:4, and IV:6).

All patients had had myoclonic jerks continuously or at least for some time during the course of their disease except for patient III/IV:3, who had only writer's cramp. Relief of myoclonic jerks by alcohol intake is reported by the patients examined. Fourteen individuals had dystonic features of different intensity and location (torticollis and/or writer's cramp) in addition to myoclonus.

### Exclusion of Mutations in the DRD 2 Gene

To exclude pathogenic mutations in the coding sequence of the DRD2 gene, we sequenced all seven exons in 2 index patients from each family (patients sequenced are shown with + in the Table). No mutations could be identified.

In addition, to exclude cosegregation of mutations in regulatory sequences of the D2 dopamine receptor gene with the disease, we performed linkage analysis with two polymorphic markers flanking in the DRD2 gene and one intragenic CA repeat polymorphism

Fig 1. Four German pedigrees with myoclonus dystonia syndrome. The symbols of family members affected are shaded black. In family II only the part of the pedigree with relation to the affecteds is shown (for the complete pedigree see Gasser et al.<sup>3</sup>). Asterisks indicate individuals typed with polymorphic markers.

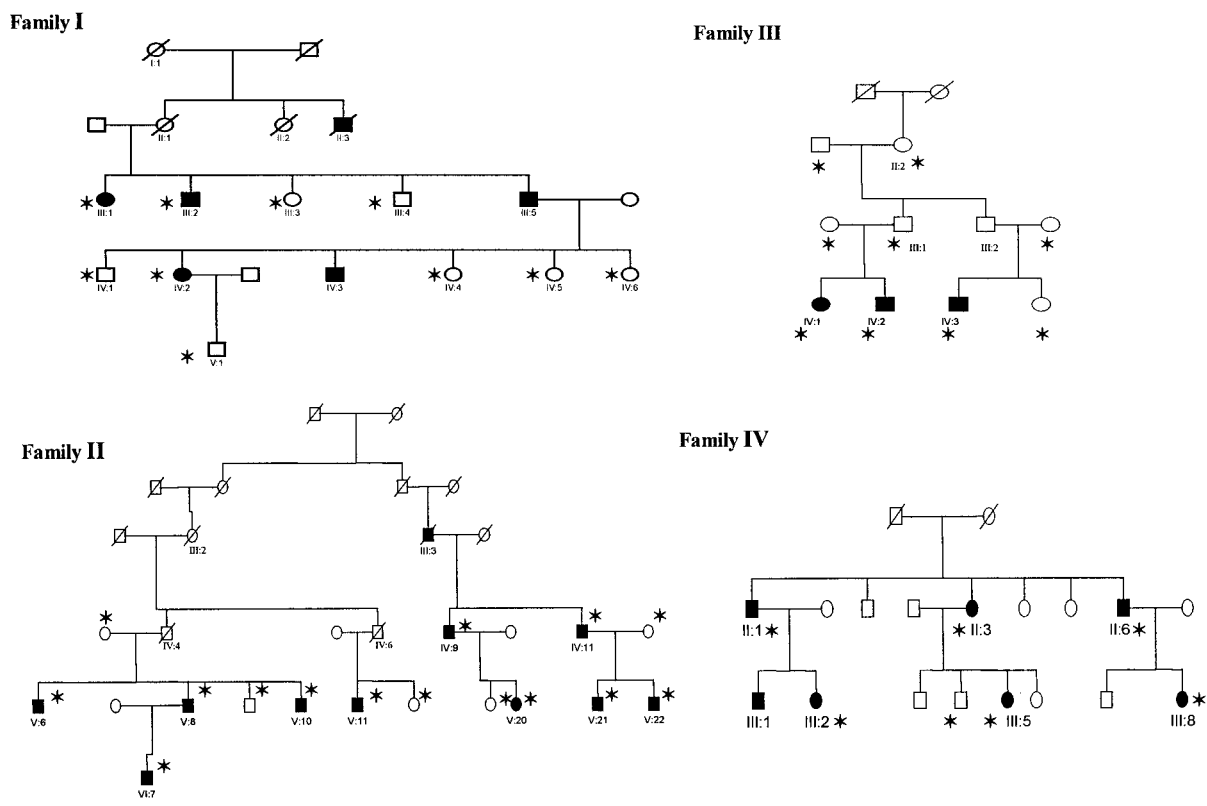


Table. Clinical Characteristics of Myoclonus-Dystonia Patients

| Individual |                        |     | Age at onset (yr) | Mc  | Tc  | Wc | DRD2 sequencing | Remarks  |
|------------|------------------------|-----|-------------------|-----|-----|----|-----------------|--|
| Family     | Generation, Individual | Sex |                   |     |     |    |                 |  |
| I          | III: 1                 | f   | ?                 | +   |     |    |                 |  |
| I          | III: 2                 | m   | ?                 | +   |     |    |                 |  |
| I          | III: 5                 | m   | 6                 | +   | +   |    | +               |  |
| I          | IV: 2                  | f   | 18                | +   | +   | +  | +               |  |
| I          | IV: 3                  | m   | Early childhood   | +   | +   | +  |                 | Alcohol abuse                                    |
| II         | III: 3                 | f   | ?                 | +   |     |    |                 | Deceased, by family history                      |
| II         | IV: 9                  | m   | ?                 | +   | +   | +  |                 |  |
| II         | IV: 11                 | m   | ?                 | +   |     |    | +               |  |
| II         | V: 6                   | m   | 10                | +   |     |    |                 | Left stereotactic thalotomy                      |
| II         | V: 8                   | m   | 12                | +   |     |    | +               |  |
| II         | V: 10                  | m   | 9                 | +   |     |    |                 | Bilateral stereotactic thalotomy                 |
| II         | V: 11                  | m   | ?                 | (+) | +   | +  |                 | Not considered to suffer from "family condition" |
| II         | V: 20                  | f   | 4                 | +   | (+) | +  |                 |  |
| II         | V: 21                  | m   | 9                 | +   |     |    |                 |  |
| II         | V: 22                  | m   | 11                | +   | +   | +  |                 |  |
| II         | VI: 7                  | m   | 6                 | +   |     |    |                 |  |
| III        | IV: 1                  | f   | Childhood         | +   | +   |    | +               |  |
| III        | IV: 2                  | m   | Childhood         | +   |     |    | +               |  |
| III        | IV: 3                  | m   | Childhood         | -   |     | +  |                 |  |
| IV         | II: 1                  | m   | Early childhood   | +   | +   | +  |                 |  |
| IV         | II: 3                  | f   | 3                 | +   | +   | +  | +               |  |
| IV         | II: 6                  | m   | Childhood         | +   | +   | +  | +               |  |
| IV         | III: 1                 |     | No data           |     |     |    |                 |  |
| IV         | III: 2                 | f   | 6                 | +   | +   | +  |                 |  |
| IV         | III: 5                 | f   | Childhood         | +   |     | +  |                 |  |
| IV         | III: 8                 | m   | 2                 | +   |     | +  |                 |  |

Mc, myoclonus; Tc, torticollis; Wc, writers cramp. (+), mild or transient phenotype.

(D11S2000, DRD2, and D11S897). No evidence for linkage was found.

#### Fine Mapping of the Chromosome 7q21 Locus

Linkage was evaluated to 12 microsatellite markers spanning a 22.1 cM region on chromosome 7q21–31 as reported by Nygaard et al.<sup>6</sup> Family I provided little information with a maximum multipoint lod score of 0.23. However, the maximum lod score was only 0.3, using the affecteds-only simulation with a completely linked, highly polymorphic (PIC 0.87) marker. Thus, this family may in fact be linked.

In pedigree II–IV linkage to the candidate region is supported with maximum multipoint lod scores between markers D7S652 and D7S2480 of 3.87, 0.90, and 1.21, respectively. The combined maximum multipoint lod score for all 4 families is 5.99 (Fig 2).

In family II key recombinations in individual V:6 between D7S652 and D7S1489 and individual V:10 between D7S476 and D7S2480 refined the candidate region to a 7.2 cM interval between D7S652 and D7S2480. There was no evidence of allele sharing, indicating that different mutations are likely to be causative in each family.

#### Discussion

Our data support the results of Nygaard et al<sup>6</sup> and argue for a major role of the chromosome 7q21 locus in inherited MDS. By observing key recombinations in pedigree II (affecteds V:6 and V:10), the candidate region could be refined to a 7.2 cM interval between the microsatellite markers D7S652 and D7S2480.

For this region we performed a database search (NCBI gene map [<http://www.ncbi.nlm.nih.gov/genemap>]) to identify candidate genes. While considering ion channels and neurotransmitter receptors as top candidate genes, we found no nucleotide sequences belonging to these groups. However, the gene for tachykinin 1, the precursor for substance P and neurokinin A, is located within this region; these peptides have been shown to excite neurons and evoke behavioral responses. Therefore, tachykinin 1 might be an interesting candidate gene for MDS.

The Val154Ile mutation of the DRD2 gene was excluded as a potential etiologic factor in our families. Mutations in regulatory sequences of the DRD2 gene have been excluded indirectly by linkage analysis. These results suggest that the DRD 2 receptor plays no major role in the majority of families with inherited MDS.

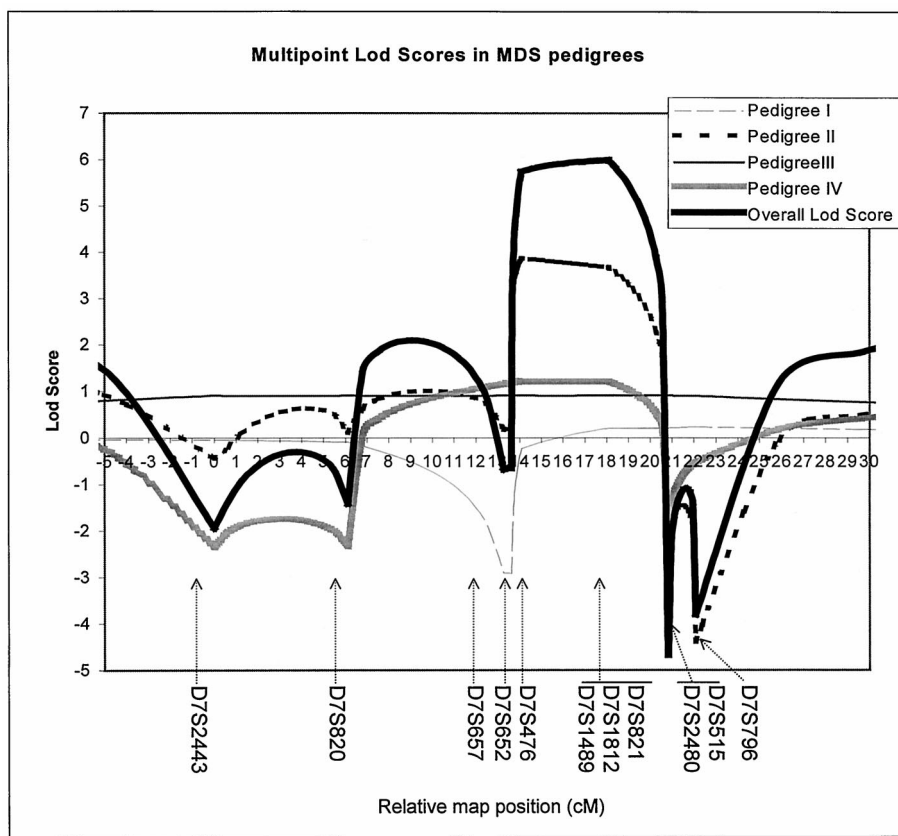


Fig 2. Multipoint lod scores on chromosome 7q21 in German MDS families. The combined maximum lod score is 5.99 between markers D7S652 and D7S2480.

Recently, psychiatric symptoms have been associated with MDS in the families reported by Klein et al<sup>5</sup> and Nygaard et al.<sup>6</sup> We found no comorbidity with depression, anxiety, or obsessive-compulsive disorders. However, most of the patients in pedigree II report a regular intake of moderate to large amounts of alcohol, which relieves their myoclonic jerks. Because all of the patients investigated are well socialized, we consider alcohol abuse as a way of learned symptomatic control and not as a specific psychiatric disorder. Recently, similar linkage results have also been reported in abstract form by Klein et al.<sup>8</sup>

This study was supported by the Myoclonus Research Foundation (USA).

We thank Doris Fuchs and Stephanie Petersen for expert technical assistance. We also thank Günther Denuschl for referral of the index patient in family II.

## References

1. Gasser T. Inherited myoclonus-dystonia syndrome. *Adv Neurol* 1998;78:325–34:325–334.
2. Quinn NP, Rothwell JC, Thompson PD, et al. Hereditary myoclonic dystonia, hereditary torsion dystonia and hereditary essential myoclonus: an area of confusion. *Adv Neurol* 1988; 50:391–401.
3. Gasser T, Bereznai B, Müller B, et al. Linkage studies in

alcohol-responsive myoclonic dystonia. *Mov Disord* 1996;12: 363–370.

4. Kurlan R, Behr J, Medved L, et al. Myoclonus and dystonia: a family study. *Adv Neurol* 1988;50:385–389.
5. Klein C, Brin MF, Kramer P, et al. Association of a missense change in the D2 dopamine receptor with myoclonus dystonia. *Proc Natl Acad Sci USA* 1999;96:5173–5176.
6. Nygaard TG, Raymond D, Chen C, et al. Localization of a gene for myoclonus-dystonia to chromosome 7q21–q31. *Ann Neurol* 1999;46:794–798.
7. O'Connell JR, Weeks DE. The VITESSE algorithm for rapid exact multilocus linkage analysis via genotype set-recoding and fuzzy inheritance. *Nat Genet* 1995;11:402–408.
8. Klein C, Kramer PL, Friedman J, et al. Myoclonus-dystonia is linked to chromosome 7q in five out of six families [abstract]. *Neurology* 2000;54(S3):A264.

# Variable Phenotype of Alzheimer's Disease with Spastic Paraparesis

Margaret J. Smith, BSc (Hons),<sup>1-3</sup> John B.J. Kwok, PhD,<sup>4</sup> Catriona A. McLean, MD,<sup>1,2</sup> Jillian J. Kril, PhD,<sup>5</sup> G. Anthony Broe, MB, BS,<sup>6</sup> Garth A. Nicholson, MB, BS, PhD,<sup>7</sup> Roberto Cappai, PhD,<sup>1,2</sup> Marianne Hallupp, BSc,<sup>4</sup> Richard G.H. Cotton, PhD,<sup>3</sup> Colin L. Masters, MD,<sup>1,2</sup> Peter R. Schofield, PhD, DSc,<sup>4</sup> and William S. Brooks, MB, BS, MPH<sup>5</sup>

---

**A variant form of Alzheimer's disease (AD), in which spastic paraparesis (SP) precedes dementia, is characterised by large, noncored, weakly neuritic A $\beta$ -amyloid plaques resembling cotton wool balls and is caused by genomic deletion of presenilin 1 exon 9. A pedigree with a 5.9 kb exon 9 deletion shows a phenotypic spectrum including subjects with typical AD or with SP and numerous cotton wool plaques. In SP subjects, dementia onset is delayed and modified. This phenotypic variation suggests that modifying factors are associated with exon 9 deletions.**

---

Ann Neurol 2001;49:125-129

---

Alzheimer's disease (AD) is the most common form of dementia. Mutations in one of three genes, the amyloid precursor protein (APP) gene, the presenilin 1 (PS1), and the presenilin 2 (PS2) genes, give rise to early-onset familial AD.<sup>1</sup> Spastic paraparesis (SP), or progressive spasticity of the lower limbs, frequently occurs on a hereditary background and has been described either alone ("pure" SP) or in association with other conditions ("complicated" SP). Several reports have described SP in families with dementia.<sup>2-7</sup> The neuropathological features in many of these pedigrees are typical of AD, although other forms exist.<sup>7</sup> Mutations reported in familial AD with SP have been confined to PS1, with three pedigrees having a deletion of exon 9<sup>2,3,5</sup> and a single

---

From the <sup>1</sup>Department of Pathology, The University of Melbourne, Melbourne, <sup>2</sup>Mental Health Research Institute, Parkville, and <sup>3</sup>Mutation Research Centre, St. Vincent's Hospital, Fitzroy, Victoria; <sup>4</sup>Garvan Institute of Medical Research, Darlinghurst, Sydney; <sup>5</sup>Centre for Education and Research on Ageing, University of Sydney, and Concord Hospital, Concord; <sup>6</sup>Prince of Wales Hospital, Randwick; and <sup>7</sup>Molecular Medicine Laboratory, Concord Hospital, Concord, New South Wales, Australia.

The first two authors contributed equally to this work.

Received May 26, 2000, and in revised form Sep 7. Accepted for publication Sep 10, 2000.

Address correspondence to Prof Schofield, Garvan Institute of Medical Research, 384 Victoria Street, Darlinghurst, Sydney, NSW 2010 Australia. E-mail: p.schofield@garvan.unsw.edu.au

case having a novel PS1 mutation (R278T).<sup>2</sup> In the recently reported Finn2 pedigree,<sup>5,8</sup> 10 of 14 individuals with dementia also had SP. Examination of the brains of three subjects, two with and one without SP, revealed many large, diffuse, noncored, and weakly neuritic plaques (resembling cotton wool balls) in all three cases, together with neurofibrillary tangles (NFTs) and pronounced congophilic angiopathy.<sup>8</sup> This variant form of AD with SP resulted from a 4.6 kb genomic deletion of PS1 exon 9.<sup>9</sup> Exon 9 deletions are exceptional in that the resultant protein is not subject to endoproteolytic cleavage,<sup>10</sup> and they strongly promote an increased production of A $\beta$ 42(43),<sup>11</sup> a major component of amyloid plaques in AD.

## Materials and Methods

### *Immunohistochemistry*

Formalin-fixed sections of temporal cortex were sectioned at 10  $\mu$ m and treated with 80% formic acid for antigen retrieval. Primary antibodies used were monoclonal antibody 1E8, which recognizes epitopes between amino acids 18 and 22 of  $\beta$ -amyloid (SmithKline Beecham, U.K.), and a polyclonal rabbit antibody to tau (Dako, Glostrup, Denmark). Immunoreactivity was developed with secondary antibody linked to horseradish peroxidase (using 3,3'-diaminobenzidine as chromagen).

### *RT-PCR Analysis of PS1 mRNA*

Total RNA was extracted from frozen brain using Trizol reagent (Gibco-BRL, Grand Island, NY) or from lymphocytes using SV Total RNA Isolation System (Promega, Madison, WI). Brain RNA was screened for mutations by RT-PCR, followed by CCM analysis.<sup>12</sup> Lymphocyte RNAs were examined for exon 9 deletion by RT-PCR using primers ex8F11 (5'-TCCCTGAATGGACTGCGTGGCTC-3') and ex10R18 (5'-GCTTCCGGGTCTCCTTCTGCCAT-3').

### *Genomic Analysis of PS1 Gene*

Microsatellite primers were from the Genome Database [http://gdbwww.gdb.org]. PCR primers for analysis of deletion breakpoints were PS1(Intron8)-F (5'-TGGGAGGTAGAAGC-AGGAGGATTG-3'), PS1(Intron9)-F (5'-CGGAAGTAGAA-GTTACATTGG-3'), and PS1(Intron9)-R (5'-GCAAAATGT-AACTCTTCTGTCTTCCCAG-3').

## Results and Discussion

### *Clinical Features*

We report a three-generation early-onset AD pedigree (Aus-1) with 13 affected subjects who have developed either dementia or SP or both (Fig 1a, Table). The first known affected individual (I:1) was admitted to a psychiatric hospital with dementia at age 53 years. A gait abnormality was not recorded, although she had brisk reflexes. She died at age 58 years with advanced dementia. Seven of her 10 children developed presenile dementia, although none had SP. II:10 had AD with onset at age 46 years and died at age 52 years. Four of

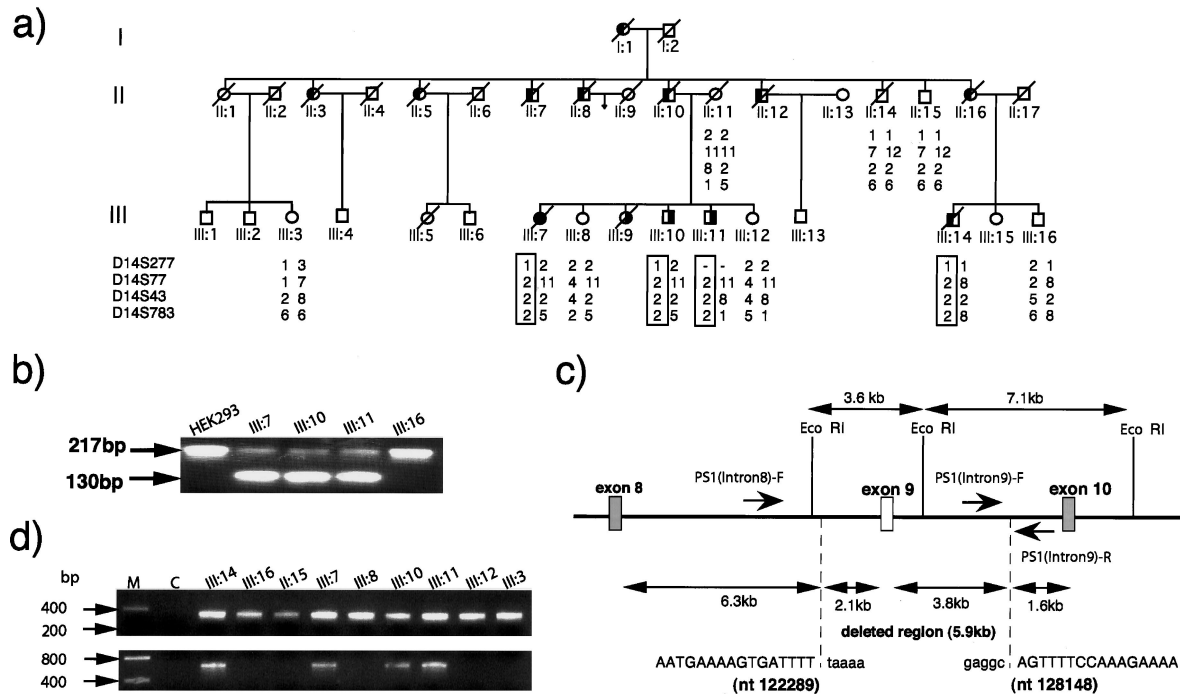


**Fig 1. Genetics of dementia and spastic paraparesis in pedigree Aus-1.** (a) Variable presentation of clinical phenotypes. Symbols filled on the left side indicate dementia without spastic paraparesis; symbols filled on the right side indicate spastic paraparesis without apparent dementia; solid symbols indicate spastic paraparesis with dementia. Haplotype analysis using four microsatellite markers within 2 cM of the PS1 gene reveal a common disease haplotype (boxed) detected in the affected individuals. The pedigree has been previously referred to as EOFAD-1.<sup>4</sup> (b) RT-PCR analysis of PS1 cDNA in three affected individuals reveals a smaller PCR product (130 bp) corresponding to the exon 9 deleted sequence. The 217 bp PCR product was amplified from an unaffected individual and control HEK293 cells expressing the entire PS1 cDNA. (c) Genomic structure of the PS1 gene deletion. A 5.9 kb portion of the PS1 gene surrounding exon 9 is deleted in affected individuals (dashed lines). This results in the generation of a novel 4.8 kb EcoRI restriction fragment. The nucleotide sequences flanking the deleted region are indicated with capital letters. No direct alignment of repetitive sequence elements flanks the breakpoint; the closest repetitive sequence is a single MER58B element located 60 bp from the breakpoint. Some localised sequence complementarity is seen at the site of the breakpoint. The nucleotide number corresponds to PS1 gene sequence (Genbank accession AF109907). (d) PCR primers PS1(Intron8)-F and PS1(Intron9)-R were used to amplify a 640 bp product, which contains the deletion breakpoints, from genomic DNAs from affected individuals (top). PS1(Intron9)-F and PS1(Intron9)-R amplify a 346 bp product from all individuals (bottom). PCR products were electrophoresed on a 1.8% agarose gel with Low DNA Mass Ladder (GibcoBRL) as size marker (M). C is the no-template DNA control.

his offspring developed SP during the fifth decade of life. III:7 developed impaired memory, language, and executive function. Her motor symptoms occurred at about the same time as the successful surgical removal of a cerebellopontine angle meningioma but continued to progress, with the development of dementia, myoclonus, and seizures. She died at age 63 years in an advanced stage of dementia and immobility. Three siblings also developed SP. III:9 developed symptoms at age 50 years and died of breast cancer at age 53 years but was considered not to have dementia. The remaining 2 affected siblings are severely disabled by SP. III:10 was admitted to a nursing home because of physical disability after 10 years of symptoms. He is currently 58 years old and has dysarthria and dysphonia, with cognitive and motor slowing. III:11 has

shown no significant cognitive decline on repeated neuropsychological testing but has also developed dysarthria, dysphonia, and swallowing difficulties. At age 54 years, he is independently mobile in a wheelchair and is not demented. The clinical features in this branch of the pedigree are in contrast to those of III:14, whose symptoms began at age 36 years and had the aggressive form of typical AD, with no evidence of SP, and he died at age 46 years.

#### Neuropathology

The neuropathologic features of the pedigree are similarly varied (Table). Review of archival photographs and limited slides of II:7 and II:12 showed generalised cortical atrophy, more marked in the hippocampus and inferior temporal cortex. Similar microscopic findings

Table. Summary of Clinical and Neuropathological Features of Affected Pedigree Members

| Subject | Sex | Age of onset (yrs) | Duration (yrs) | Clinical findings at presentation | Neuropathology                 |                                   |                                       |     |                  |
|---------|-----|--------------------|----------------|-----------------------------------|--------------------------------|-----------------------------------|---------------------------------------|-----|------------------|
|         |     |                    |                |                                   | Congophilic amyloid angiopathy | Cortico-spinal tract degeneration | $\beta$ -Amyloid plaques <sup>a</sup> |     | Cortical atrophy |
|         |     |                    |                |                                   |                                | Cored                             | Variant <sup>b</sup>                  |     |                  |
| I:1     | F   | 53                 | 5              | Dementia <sup>c</sup>             |                                |                                   |                                       |     |                  |
| II:3    | F   | 36                 | 7              | Dementia <sup>d</sup>             |                                |                                   |                                       |     |                  |
| II:5    | F   | 47                 | 2              | Dementia                          |                                |                                   | +                                     |     | +                |
| II:7    | M   | 52                 | 4              | Dementia                          | h                              | –                                 | +                                     | +   | +                |
| II:8    | M   | 47                 | 5              | Dementia <sup>e</sup>             |                                |                                   |                                       |     |                  |
| II:10   | M   | 46                 | 6              | Dementia                          |                                |                                   |                                       |     |                  |
| II:12   | M   | 41                 | 5              | Dementia <sup>f</sup>             | h                              | –                                 | –                                     | +   | +                |
| II:16   | F   | 39                 | 8              | Dementia                          |                                |                                   |                                       |     |                  |
| III:7   | F   | 54                 | 9              | Dementia and spastic paraparesis  | +                              | +                                 | +                                     | ++  | +                |
| III:9   | F   | 50                 | 3 <sup>g</sup> | Spastic paraparesis               | +                              | +                                 | –                                     | +++ | –                |
| III:10  | M   | 46                 | 11 (alive)     | Spastic paraparesis               |                                |                                   |                                       |     |                  |
| III:11  | M   | 48                 | 6 (alive)      | Spastic paraparesis               |                                |                                   |                                       |     |                  |
| III:14  | M   | 36                 | 10             | Dementia                          | +                              | –                                 | +++                                   | –   | +                |

<sup>a</sup> $\beta$ -Amyloid plaque frequency (+ to +++).

<sup>b</sup>Large, noncored, weakly neuritic plaques.

<sup>c</sup>Initial presentation of suspiciousness, hallucinations, confusion, and deficits in memory and language.

<sup>d</sup>Gait was normal.

<sup>e</sup>Gait was clumsy but reflexes were normal.

<sup>f</sup>Seizures were also present.

<sup>g</sup>Died of breast cancer.

<sup>h</sup>Unable to assess from archival material.

Subject II: 14, who does not have the disease haplotype, died aged 79 years with mild cognitive impairment. Neuropathology showed occasional cored plaques but no large plaques and no significant cortical neuritic pathology, demonstrating that variant neuropathology is seen only in individuals with the PS1 exon 9 deletion.

in both subjects included numerous large cortical plaques, predominantly lacking cores, seen in all laminae. In III:14, the atrophic brain showed widespread and marked neuronal loss and NFT formation. Frequent A $\beta$ -immunoreactive plaques were seen that contained tau-immunoreactive neuritic processes and moderate numbers of central amyloid cores (Fig 2a). A diagnosis of AD was made based on CERAD criteria.<sup>13</sup> This is in contrast to the case with III:7, in whom frequent large plaques were seen, within which fine tau-immunoreactive processes were evident, as were very occasional cores. Less marked neuronal loss was also seen compared to III:14. Sparse numbers of cortical tau-immunoreactive NFTs were evident (Fig 2a). A diagnosis of AD was made. Of particular interest are the lesions in III:9, who had SP only and died prematurely of breast cancer. The brain was macroscopically normal. Within the cortex, widespread, large, noncored plaques were seen. There was no significant neuronal loss or NFT formation (Fig 2a). These changes do not fulfill the CERAD diagnostic criteria for AD. The large plaques observed in III:7 and III:9 are similar to “cotton wool” plaques.<sup>8</sup> Corticospinal tract degeneration was also present in SP subjects III:7 and III:9 (Table, Fig 2b).

### Genetic Analysis

Coding sequence or splice site mutations in the PS1 gene were not detected.<sup>2</sup> However, a common disease haplotype was shared by all affected individuals, suggesting that PS1 is the causative locus (Fig 1a). RT-PCR analysis was performed from total RNA extracted from frozen brain of III:14. Chemical cleavage of mismatch analysis<sup>12</sup> revealed a deletion in the 3' end of the PS1 gene. Sequencing of the RT-PCR product revealed the absence of exon 9. RT-PCR analysis of RNA extracted from lymphocytes from three other affected individuals (III:7, III:10, and III:11, all with SP), confirmed that exon 9 was also deleted (Fig 1b). Hybridisation of an intron 9 probe to EcoRI-digested DNAs from the pedigree revealed a novel 4.9 kb band in affected individuals. Correlation with known EcoRI sites suggested a 5.9 kb deletion of genomic sequences flanking exon 9 (Fig 1c). To define the deletion precisely, intronic PCR using primers PS1(Intron8)-F and PS1(Intron9)-R amplified a 640 bp product from affected individuals (III:7, III:10, III:12, and III:14) but not from five unaffected individuals; all DNAs amplified a control 346 bp PCR product from intron 9 (Fig 1d). Sequence analysis of the 640 bp product confirmed the juxtaposition of intron 8 and 9 sequences by a 5.9

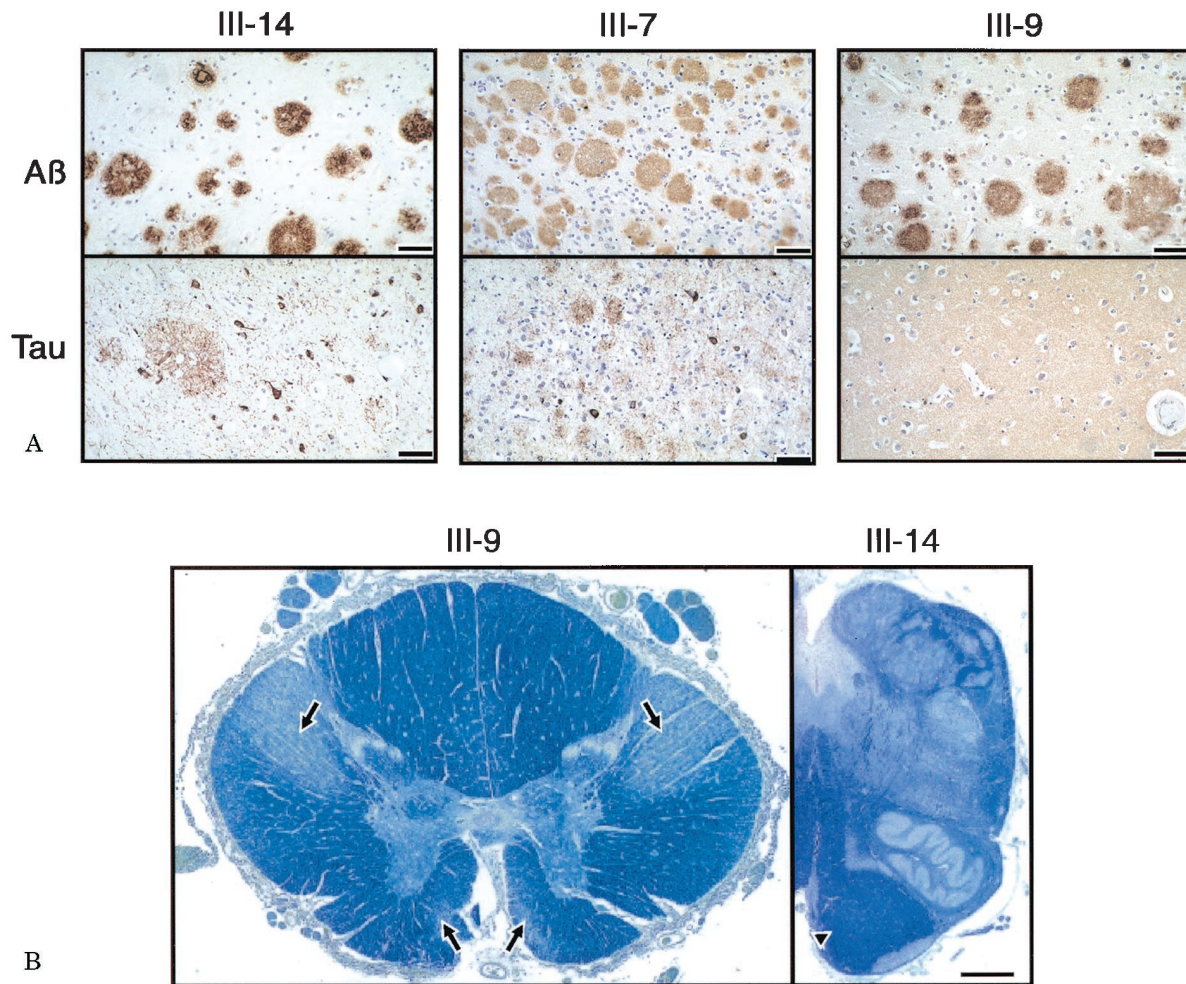


*Fig 2. Neuropathology of Aus-1 pedigree members. (a) A $\beta$ -amyloid (upper panel) and tau (lower panel) immunoreactivity in the temporal cortex of subjects III:14, III:7, and III:9 is illustrated. III:14 shows moderate numbers of A $\beta$ -amyloid plaques in the cortex, some of which show central cores. Numerous tau-immunoreactive neurofibrillary tangles (NFTs) and neuritic threads (NTs) are seen in the neuropil as are plaques outlined by the deposition of tau neuritic processes. III:7 shows numerous A $\beta$  diffuse plaques of varying size in all layers of the cortex. There is minimal evidence of central cores. The tau studies show that there are moderate numbers of NFTs and background NTs with weakly circumscribed plaques outlined by a localised concentration of tau-immunoreactive neuritic processes. III:9, who had SP but was not demented, died of breast cancer. Her cortex shows moderate numbers of A $\beta$  plaques of varying size. No plaque cores are seen. There is no evidence of any tau immunoreactivity. (b) Myelin staining in the corticospinal tract using the Luxol fast blue method. III:9 shows degeneration in the spinal cord as shown by secondary demyelination of the anterior and lateral corticospinal tracts (black arrows). III:14 shows a section of medulla showing no evidence of corticospinal tract degeneration (arrowhead). Scale bars = 50  $\mu$ m in (a); 2.5mm in (b).*

kb deletion spanning exon 9 (Fig 1c). Neither breakpoint matches the breakpoints of the 4.6 kb deletion seen in Finnish pedigrees,<sup>9,14</sup> and sequence comparisons do not support repetitive element-mediated deletions.<sup>14</sup>

SP has been observed in one branch of the Aus-1 pedigree (Fig 1a), whereas the Finn2 pedigree shows an apparent autosomal dominant inheritance through three generations.<sup>5,8</sup> A finding of brisk reflexes in the unaffected parent (II:11) led to the suggestion that paraparesis resulted from an incompletely penetrant mutation. Other causes of SP were considered, including recessive forms; however, mutations in the paraple-

gin gene at 16q24.3 (SPG-7)<sup>14</sup> were not found for III:10. Adrenoleukodystrophy was considered,<sup>15</sup> but plasma VLCFA levels were normal in III:11, who has severe paraparesis. On clinical grounds, the onset in middle age and the lack of accompanying features, such as deafness or pigmentary abnormalities, made many of the complicated SP syndromes unlikely. We conclude that the PS1 exon 9 deletion is the most likely explanation for both SP and AD in this family. The pattern of segregation of SP and dementia in this and other pedigrees<sup>8,9,16</sup> is consistent with the coinheritance of phenotypic modifier genes.

### Implications

The clinical, genetic, and neuropathological findings in this and similar families raise issues with wider implications for our understanding of AD. First, PS1 mutations characteristically result in a severe form of AD<sup>1</sup> with a mean age at onset of 44 years and presentation as early as the mid-20s.<sup>17,18</sup> Despite PS1 exon 9 deletions giving rise to very high levels of A $\beta$ 42(43) in vitro,<sup>11</sup> AD pedigrees with SP and a PS1 exon 9 deletion have a later mean age of onset, ranging from 48<sup>3</sup> to 51<sup>8</sup> years. In Aus-1, 3 of the 4 individuals who developed SP remained dementia-free for up to 10 years. This delay in the age of onset of dementia is not explained by the inheritance of a protective apolipoprotein E  $\epsilon$ 2 allele;<sup>19</sup> the affected individuals have either  $\epsilon$ 3/ $\epsilon$ 3 or  $\epsilon$ 3/ $\epsilon$ 4 genotypes. Second, the presence of the variant cotton wool plaques, as seen in the Finn2 pedigree,<sup>8</sup> suggests that the major determinant of dementia is not the dense amyloid deposits but rather is upstream in the pathogenic cascade.<sup>1</sup> In both these pedigrees, the motor neurons and their axons in the corticospinal tracts appear to be more acutely vulnerable than the regions usually affected in AD. Third, III:9, dying of breast cancer, highlights a key phenomenon with respect to the pathogenesis of AD, namely, the enigmatic interrelation of A $\beta$  and tau. In III:9, A $\beta$  plaques are seen in the absence of neuronal loss, NFT deposition, and cognitive decline. An interpretation of these findings is that the relationship between plaques and NFTs is, in part, a temporal phenomenon, with A $\beta$  deposition preceding tau deposition in the neocortex.<sup>20</sup> Understanding the phenotypic heterogeneity seen in association with PS1 exon 9 deletions may provide important clues to the factors involved in the temporal sequence of events and the topography of AD. This may provide insights leading to the development of future therapeutic strategies.

---

This study was supported by the National Health and Medical Research Council (Australia) through project and block grants; the Network of Brain Research Into Mental Disorders and an Australian Postdoctoral Fellowship in Dementia; a research grant from the Australian Department of Veterans' Affairs; and the Medical Foundation, University of Sydney.

The authors thank Drs H. Creasey and M. Halmagyi for clinical details, Dr R. Pamphlett for providing neuropathological specimens, Dr Giorgio Casari for screening for SPG7 mutations, Dr S.M. Forrest and M.A. Knight for advice on mutation screens, and Prof K. Beyreuther for collaborative discussions.

### References

1. Price DL, Sisodia SS. Mutant genes in familial Alzheimer's disease and transgenic models. *Annu Rev Neurosci* 1998;21:479–505.
2. Kwok JBJ, Taddei K, Hallupp M, et al. Two novel (M233T and R278T) presenilin-1 mutations in early-onset Alzheimer's disease and preliminary evidence for association of presenilin-1 mutations with a novel phenotype. *Neuroreport* 1997;8:1537–1542.
3. Sato S, Kamino K, Miki T, et al. Splicing mutation of presenilin-1 gene for early-onset familial Alzheimer's disease. *Hum Mutat* 1998;(Suppl 1):S91–S94.
4. van Bogaert L, Maere M, de Smedt E. Sur les formes familiales précoces de la maladie d'Alzheimer. *Monatsschr Psychiatr Neurol* 1940;102:249–301.
5. Verkkoniemi A, Somer M, Rinne JO, et al. Variant Alzheimer's disease with spastic paraparesis: clinical characterization. *Neurology* 2000;54:1103–1109.
6. Sodeyama N, Shimada M, Uchihara T, et al. Spastic tetraplegia as an initial manifestation of familial Alzheimer's disease. *J Neurol Neurosurg Psychiatr* 1995;59:395–399.
7. Vidal R, Frangione B, Rostagno A, et al. A stop-codon mutation in the BRI gene associated with familial British dementia. *Nature* 1999;399:776–781.
8. Crook R, Verkkoniemi A, Perez-Tur J, et al. A variant of Alzheimer's disease with spastic paraparesis and unusual plaques due to deletion of exon 9 of presenilin 1. *Nat Med* 1998;4:452–455.
9. Prihar G, Verkkoniemi A, Perez-Tur J, et al. Alzheimer disease PS-1 exon 9 deletion defined. *Nat Med* 1999;5:1090.
10. Thinakaran G, Borchelt DR, Lee MK, et al. Endoproteolysis of presenilin 1 and accumulation of processed derivatives in vivo. *Neuron* 1996;17:181–190.
11. Mehta ND, Refolo LM, Eckman C, et al. Increased A $\beta$ 42(43) from cell lines expressing presenilin 1 mutations. *Ann Neurol* 1998;43:256–258.
12. Smith MJ, Humphrey KE, Cappai R, et al. Correct heteroduplex formation for mutation detection analysis. *Mol Diagn* 2000;5:67–73.
13. Mirra SS, Heyman A, McKeel D, et al. The Consortium to Establish a Registry for Alzheimer's Disease (CERAD). Part II. Standardization of the neuropathologic assessment of Alzheimer's disease. *Neurology* 1991;41:479–486.
14. Casari G, De Fusco M, Ciarmatori S, et al. Spastic paraplegia and OXPHOS impairment caused by mutations in paraplegin, a nuclear-encoded mitochondrial metalloprotease. *Cell* 1998;93:973–983.
15. O'Neill BP, Swanson JW, Brown FR 3rd, et al. Familial spastic paraparesis: an adrenoleukodystrophy phenotype? *Neurology* 1985;35:1233–1235.
16. Hiltunen M, Helisalmi S, Mannermaa A, et al. Identification of a novel 4.6-kb genomic deletion in presenilin-1 gene which results in exclusion of exon 9 in a Finnish early onset Alzheimer's disease family: an Alu core sequence-stimulated recombination? *Eur J Hum Genet* 2000;8:259–266.
17. Rohan de Silva HA, Patel AJ. Presenilins and early-onset familial Alzheimer's disease. *Neuroreport* 1997;8:i–xii.
18. Taddei K, Kwok JBJ, Kril JJ, et al. Two novel presenilin-1 mutations (Ser169Leu and Pro436Gln) associated with very early onset Alzheimer's disease. *Neuroreport* 1998;9:3335–3339.
19. Corder EH, Saunders AM, Risch NJ, et al. Protective effect of apolipoprotein E type 2 allele for late onset Alzheimer disease. *Nat Genet* 1994;7:180–184.
20. Thal DR, Rub U, Schultz C, et al. Sequence of Abeta-protein deposition in the human medial temporal lobe. *J Neuropathol Exp Neurol* 2000;59:733–748.

# Distal Anterior Compartment Myopathy: A Dysferlin Mutation Causing a New Muscular Dystrophy Phenotype

Isabel Illa, MD,<sup>1</sup> Carme Serrano-Munuera, MD,<sup>1</sup> Eduard Gallardo, PhD,<sup>1</sup> Adriana Lasa, PhD,<sup>2</sup> Ricardo Rojas-García, MD,<sup>1</sup> Jaume Palmer, MD,<sup>3</sup> Pia Gallano, PhD,<sup>3</sup> Montserrat Baiget, PhD,<sup>3</sup> Chie Matsuda, PhD,<sup>4</sup> and Robert H. Brown, MD, PhD<sup>4</sup>

**We report a family with a new phenotype of autosomal recessive muscle dystrophy caused by a dysferlin mutation. The onset of the illness is distal, in the muscles of the anterior compartment group. The disease is rapidly progressive, leading to severe proximal weakness. Muscle biopsy showed moderate dystrophic changes with no vacuoles. Dysferlin immunostaining was negative. Gene analysis revealed a frameshift mutation in the exon 50 (delG5966) of the DYSF gene. This phenotype further demonstrates the clinical heterogeneity of the dysferlinopathies.**

Ann Neurol 2001;49:130–134

The distal myopathies are a heterogeneous group of disorders clinically characterized by primary involvement of distal muscles and by myopathic features in the muscle biopsy.<sup>1–6</sup> Miyoshi and Nonaka myopathies, both with early-adult onset, are the two major distal myopathies with autosomal recessive inheritance and onset in the legs. Miyoshi myopathy begins in the posterior compartment, creatine kinase (CK) level is markedly elevated and muscle biopsy reveals dystrophic changes.<sup>7</sup> Nonaka myopathy is characterized by onset in the anterior compartment, mildly elevated CK level and by rimmed vacuoles in the muscle biopsy.<sup>8,9</sup> These two distal myopathies map to different chromosomes, which confirms that they are indeed different muscle diseases. Nonaka myopathy links to chromosome 9p1-

From the <sup>1</sup>Neuromuscular Diseases Section, Department of Neurology, <sup>2</sup>Department of Genetics and <sup>3</sup>Department of Radiology, Hospital Santa Creu i Sant Pau, Universitat Autònoma de Barcelona (UAB), Barcelona, Spain; and the <sup>4</sup>Day Neuromuscular Research Laboratory, Charlestown, MA.

Received Apr 20, 2000, and in revised form Sep 21. Accepted for publication Sep 21, 2000.

Address correspondence to Dr Illa, Department of Neurology, Hospital Santa Creu i Sant Pau, Av Pare Claret 167, Barcelona 08025, Spain. E-mail: iilla@hsp.santpau.es

q1,<sup>10</sup> whereas Miyoshi myopathy has been associated with mutations in the dysferlin gene.<sup>11</sup>

Mutations in the dysferlin gene have recently been described in the limb girdle muscular dystrophy type 2B (LGMD2B), confirming the previous hypothesis that both this entity and Miyoshi myopathy arise from the same gene defect.<sup>12,13</sup> The term *dysferlinopathy* has been suggested to include the different muscle dystrophies with mutations in the dysferlin gene.<sup>11</sup>

We describe a family with a rapidly progressive muscular dystrophy with onset in the anterior tibial muscles. The phenotype of this autosomal recessive distal myopathy is different from those of Miyoshi and Nonaka myopathies. The disease has been linked to the 2p13 locus<sup>14</sup> and a homozygous mutation in the dysferlin gene has been confirmed.<sup>11</sup>

## Subjects and Methods

### Subjects

We describe 4 members (IV:9, IV:10, IV:11, and IV:17) of a consanguineous family from the Spanish Mediterranean coast (pedigree is shown in Fig 1). Another 32 members of the kindred were also examined and found to be normal. All subjects gave their informed consent.

The 4 patients and 32 family members were examined according to a standardized protocol to determine clinical features, age and symptoms at onset, and disease duration. The pattern of muscle involvement and its progression was determined by neurological examination using the Medical Research Council (MRC) scale. Needle electromyography (EMG) and nerve conduction studies were performed in the patients and in their parents (III:6, III:7, and III:11). Cardiac and pulmonary function tests were performed in the four patients.

### Muscle Biopsy

Muscle biopsies from the patients were processed for muscle-enzyme histochemistry and immunocytochemistry (immunoperoxidase technique), as previously described.<sup>15</sup> Disease control biopsies included patients with other muscular dystrophies (Duchenne dystrophy, LGMD 2C and LGMD 2D, and Miyoshi and Nonaka myopathies). We used primary monoclonal antibodies (10 µg/ml) to dystrophin (DYS1 and DYS2), sarcoglycans α, β, and γ (Novocastra, Newcastle, UK), desmin (Dako, Glostrup, Denmark), and a rabbit polyclonal antibody to dysferlin.<sup>16</sup>

### Magnetic Resonance Imaging

To determine the pattern of muscle involvement, magnetic resonance imaging (MRI) (transverse spin-echo T1-weighted images) of the upper and lower extremity muscles was performed in all patients except IV:9. A Magnetom 1T (Siemens, Erlangen, Germany) was used. The results were compared with those obtained in our patients with Miyoshi myopathy.

### DNA Studies

IDENTIFICATION OF DYSFERLIN MUTATIONS. Genomic DNA was amplified for all exons of the dysferlin gene by

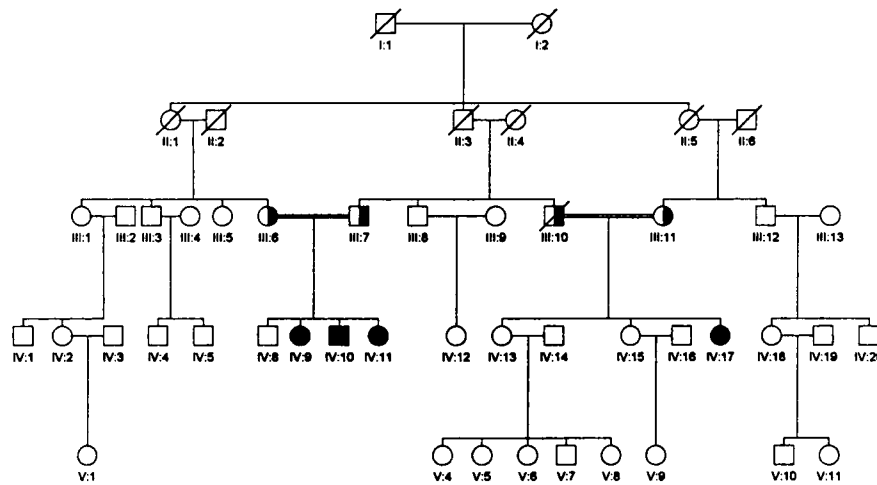


Fig 1. Pedigree. ● and ■ = affected individuals; ○ and □ = unaffected individuals.

PCR (conditions previously published). Screening for mutations in the patients was performed using the single-strand conformation polymorphism (SSCP) technique and automated sequencing.<sup>11</sup> A conformational shift was identified in the DNA of the four patients and exon 50 was directly sequenced (ABI-PRISM 310; Perkin Elmer Applied Biosystems, Foster City, CA) in patients and control subjects.

## Results

### Phenotype

The proband (IV:10) is a 40-year-old man who first presented to our neuromuscular clinic at age 28. He had previously been diagnosed with Charcot-Marie-Tooth disease. He complained of exercise-related pain from the age of 14 years. Two years later, he noticed distal leg weakness and walked with a steppage gait.

The neurologic examination, at age 28, showed severe distal symmetric weakness in the lower limbs. The anterior compartment group was the most affected (MRC 3), whereas the lower limb girdle muscles showed a mild degree of weakness (MRC 4+). Muscle strength was normal in the upper limbs except for the wrist and finger flexors (MRC 4-). Severe muscular atrophy was present in both anterior tibial muscles. In contrast, the extensor digitorum brevis muscles were normal (Fig 2). In the upper extremities, symmetric wrist and finger flexor atrophy and partial biceps brachii atrophy were noted. Both ankle and right radial reflexes were abolished and no sensory loss was found. CK level was 4006 U/l.

The course was rapidly progressive in the lower extremities, as the patient was using a wheelchair by the age of 35. The involvement of the proximal muscles was more prominent in the knee and hip flexors than in the extensors. At the age of 40 his neurological examination showed an overall MRC scale of 1 to 2 in the lower extremities, whereas in the upper extremities

the girdle muscles were still considered MRC 4-. There was no facial or bulbar muscle involvement. Muscle MRI performed at the age of 38 showed severe muscle atrophy of both upper and lower extremities, the gastrocnemius muscles being the least affected (Fig 2). In the upper extremities the degree of involvement was greater in the elbow and wrist flexor than in the extensor groups.

The other 3 patients (IV:9, IV:11, and IV:17) showed similar clinical features. The onset of the disease was between 20 and 28 years of age. All had initial isolated involvement of anterior tibial muscles followed by weakness in the proximal lower limb muscles (Fig 2). After a period of 5 to 8 years these patients also showed weakness of both wrist and finger flexor muscles, as well as involvement of the proximal muscles of the upper limbs. They lost the ability to walk after the age of 30 (31 to 50 years). Serum CK levels were highly elevated (20 to 70 times). In all patients EMG examination revealed spontaneous activity, some complex repetitive discharges in several muscles, and myopathic motor unit potentials. The results of cardiac studies were normal at the beginning of the disease, and no abnormalities have been found during a 13-year follow-up. Pulmonary function tests revealed mild reduction of vital capacity in patients IV-9 and IV-17 at the age of 35 and 34, respectively.

### Muscle Biopsies

Muscle biopsies were characteristic of a primary myopathy (Fig 3), showing fiber-size variability, central nuclei, fibers subdivided by splitting, and some infiltrates, especially in necrotic fibers undergoing phagocytosis by macrophages. Connective tissue was increased. No fiber type grouping was detected. No rimmed vacuoles or ragged red fibers were present. The immunohisto-

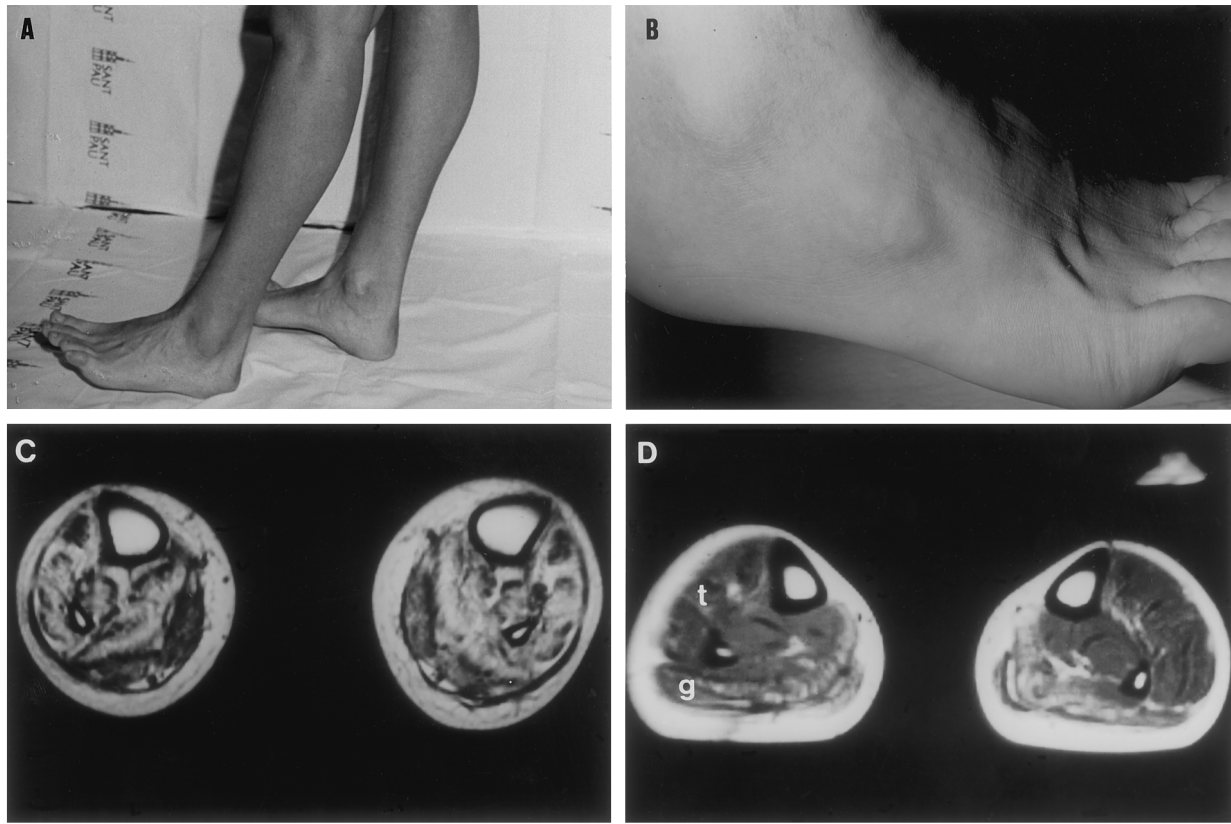


Fig 2. (A) Difficulties walking on heels in patient IV:11; (B) notice normal bulk of the extensor digitorum brevis muscle in patient IV:10. (C) Magnetic resonance imaging of lower leg muscles showing the distinct hyperintensity in the anterior tibial muscles compatible with fatty degenerative lesions in patient IV:11, (D) in contrast with the predominant posterior compartment involvement in a patient with Miyoshi myopathy. *g* = gastrocnemius; *t* = tibialis anterior.

chemical studies using antibodies to dystrophin and dystrophin-associated glycoproteins showed a normal pattern of membrane expression. No desmin deposits were observed. Dysferlin was negative in the sarcolemma of all muscle fibers (Fig 3).

#### *Dysferlin Mutations*

Nucleotide sequence analysis of the amplified products from the patients revealed a deletion of one base pair (G) in exon 50 at nucleotide position 5966–67 (codon 1865) in the dysferlin gene in the four affected individuals. The deletion creates a frameshift.

#### **Discussion**

We describe a new phenotype of distal myopathy caused by a dysferlin mutation. The clinical onset of this disease is between 14 and 28 years of age and the anterior tibial muscles are the first muscle group to be involved. This entity has a rapidly progressive course successively involving the lower and upper proximal muscles, with patients being confined to a wheelchair 11 to 22 years from onset. The cranial muscles are

spared. Serum CK level is increased 20 to 70 times the normal value and muscle histopathologic studies show moderate myopathic changes without vacuoles. The disease is inherited in an autosomal recessive pattern. The putative gene was initially mapped to chromosome 2p13 and subsequently identified as the dysferlin gene (DYSF). The delG5966 mutation in exon 50 of this gene yields an absence of dysferlin on the sarcolemma of muscle fibers in affected patients.

Our patients do not fit into any early-adulthood subtype of distal myopathy previously described.<sup>7–9</sup> The onset with anterior tibial weakness suggested a diagnosis of Nonaka myopathy; however, many differences were found. The progression of muscle involvement and the severity of the clinical course in the family described here are not common in Western patients with Nonaka myopathy.<sup>8,9,17–19</sup> The high CK level and absence of vacuoles in the muscle biopsies further differentiate both entities. In addition, recent studies have shown that the autosomal recessive distal myopathy with rimmed vacuoles described by Nonaka links to chromosome 9.<sup>10</sup>

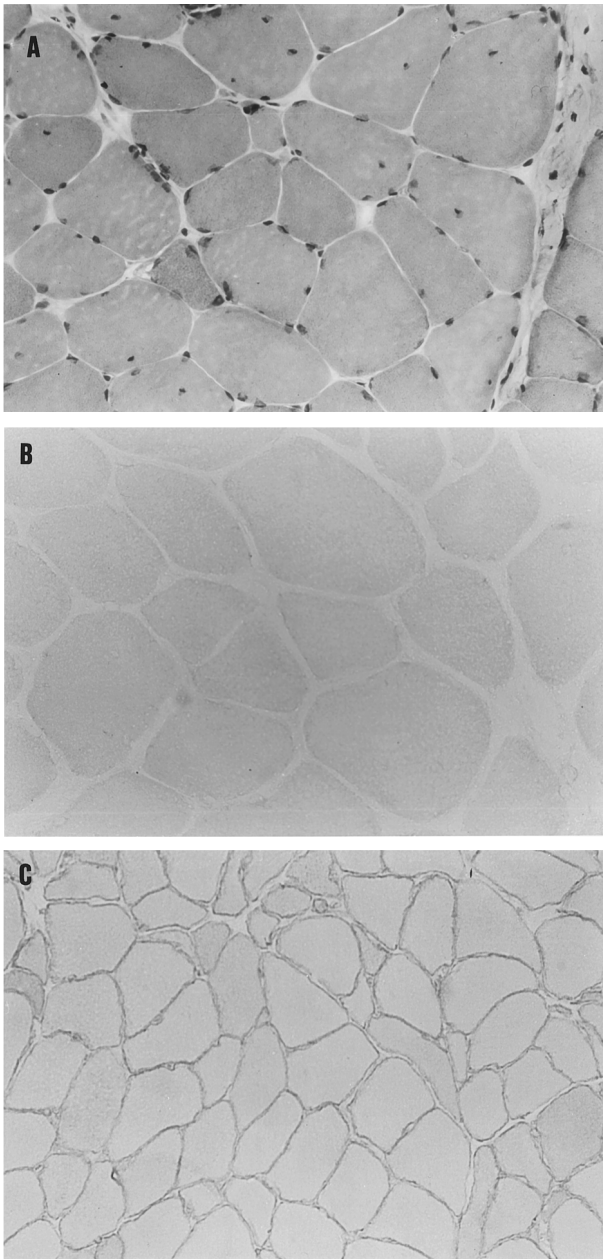


*Fig 3. (A) Hematoxylin and eosin stain of a patient with distal anterior compartment myopathy (DAT) showing dystrophic features. (B) Labeling with the anti-dysferlin rabbit polyclonal antibody Sall-1 is completely negative in all muscle fibers in a patient with DAT. (C) Immunocytochemistry with the anti-dysferlin antibody in the muscle from a patient with LGMD2C, used as a positive control, shows staining of the sarcolemma (magnification  $\times 400$  before 68% reduction).*

A diagnosis of Miyoshi myopathy, the other autosomal recessive early-onset distal myopathy, was also considered in this family because of the increased serum CK level and the dystrophic changes without vacuoles in the muscle biopsies.<sup>1,7,20</sup> However, in contrast to our patients, Miyoshi myopathy characteristically presents

with weakness of the posterior compartment of the leg with initial sparing of the anterior compartment.<sup>7</sup> The MRI findings in our patients, which showed relative sparing of the gastrocnemius muscles even at the end stage of the disease, further stress the phenotypic differences.

Myofibrillar myopathy and other forms of muscular dystrophy initially considered in the differential diagnosis were also excluded.

Genetic studies allowed the linkage to 2p13<sup>14</sup> and the identification of a homozygous mutation in exon 50 of the dysferlin gene,<sup>11</sup> indicating that the phenotype described here is a form of dysferlinopathy. Furthermore, the immunohistochemical studies confirmed that dysferlin was absent from the sarcolemma of the patients' muscle biopsies.

Molecular studies have confirmed mutations in the dysferlin gene in patients with Miyoshi myopathy or with LGMD2B, previously linked to 2p12–14, which constitute the muscular dystrophies called dysferlinopathies.<sup>11,13</sup> The 4 patients described in this report share essential clinical traits with the other two phenotypes related to dysferlin mutations: early adulthood onset, autosomal recessive inheritance, predominant involvement of the lower extremities, extremely high CK level, and dystrophic features with normal dystrophin and sarcoglycan staining, as well as the absence of dysferlin in muscle biopsies.

However, patients with dysferlin mutations present with different phenotypes defined by the distinct involvement of muscle groups. The study of this unique phenomenon would be helpful for a better understanding of the unknown underlying mechanisms which lead to a selective pattern of muscle involvement in muscular dystrophies.

---

This study was supported by FIS 99/019–01.

We thank Esther Ortiz for excellent technical assistance.

---

## References

1. Barohn RJ, Miller RG, Griggs RC. Autosomal recessive distal dystrophy. *Neurology* 1991;41:1365–1370.
2. Illa I. Miopatías distales: lecciones de la clínica y la genética. *Neurología* 2000;15:189–192.
3. Nonaka I. Distal myopathies. *Curr Opin Neurol* 1999;12:493–499.
4. Somer H. Workshop report: distal myopathies. *Neuromusc Disord* 1995;5:249–252.
5. Griggs R, Markesbery W. Distal myopathies. In: Engel A, Franzini-Armstrong C, editors. *Myology*, vol 2. New York: McGraw-Hill, 1994:1246–1257.
6. Barohn RJ, Amato AA, Griggs RC. Overview of distal myopathies: from the clinical to the molecular. *Neuromusc Disord* 1998;8:309–316.
7. Miyoshi K, Kawai H, Iwasa M, et al. Autosomal recessive distal muscular dystrophy as a new type of progressive muscular

- dystrophy: seventeen cases in eight families including an autosomal recessive case. *Brain* 1986;109:31–54.
8. Nonaka I, Sunohara N, Ishiura S, Satoyoshi E. Familial distal myopathy with rimmed vacuole and lamellar (myeloid) body formation. *J Neurol Sci* 1981;51:141–155.
  9. Nonaka I, Sunohara N, Satoyoshi E, et al. Autosomal recessive distal muscular dystrophy: a comparative study with distal myopathy with rimmed vacuole formation. *Ann Neurol* 1985;17:51–59.
  10. Ikeuchi T, Asaka T, Saito M, et al. Gene locus for autosomal recessive distal myopathy with rimmed vacuoles maps to chromosome 9. *Ann Neurol* 1997;41:432–437.
  11. Liu J, Aoki M, Illa I, et al. Dysferlin, a novel skeletal muscle gene, is mutated in Miyoshi myopathy and limb girdle muscular dystrophy. *Nat Genet* 1998;20:31–36.
  12. Bejaoui K, Hirabayashi K, Hentati F, et al. Linkage of Miyoshi myopathy (distal autosomal recessive muscular dystrophy) locus to chromosome 2p12–14. *Neurology* 1995;45:768–772.
  13. Bashir R, Britton S, Strachan T, et al. A gene related to *Caenorhabditis elegans* spermatogenesis factor *fer-1* is mutated in limb-girdle muscular dystrophy type 2B. *Nat Genet* 1998;20:37–42.
  14. Illa I, Serrano C, Gallardo E, et al. Distal anterior compartment myopathy: a new severe dystrophic phenotype linked to chromosome 2p13. *Neurology* 1998;50:A186.
  15. Illa I, Leon-Monzon M, Dalakas MC. Regenerating and denervated human muscle fibers and satellite cells express neural cell adhesion molecule recognized by monoclonal antibodies to natural killer cells. *Ann Neurol* 1992;31:46–52.
  16. Matsuda C, Aoki M, Hayashi YK, et al. Dysferlin is a surface membrane-associated protein that is absent in Miyoshi myopathy. *Neurology* 1999;53:1119–1122.
  17. Sunohara N, Nonaka I, Kamei N, Satoyoshi E. Distal myopathy with rimmed vacuole formation: a follow-up study. *Brain* 1989;112:65–83.
  18. Markesbery W, Griggs R, Herr B. Distal myopathy: electron microscopic and histochemical studies. *Neurology* 1977;27:727–735.
  19. Scoppetta C, Vaccario ML, Casali C, et al. Distal muscular dystrophy with autosomal recessive inheritance. *Muscle Nerve* 1984;7:478–481.
  20. Galassi G, Rowland LP, Hays AP, et al. High serum levels of creatine kinase: asymptomatic prelude to distal myopathy. *Muscle Nerve* 1987;10:346–350.